Stochastic Optimization of Battery Storage: An Analysis of its Potential

Master's thesis

Runar Skorge Stranden

Supervised by Dag Haugland

Geophysical Institute

University of Bergen

Acknowledgements

This thesis marks the end of a five-year master's program in Energy at the University of Bergen. My time as a student has been exciting, and I am forever grateful for all the knowledge and experiences I have gained.

I would like to express my deepest gratitude to my supervisor Dag Haugland. Completing this thesis would not have been possible without your enlightening feedback.

Further, I want to thank my employer, Volte, who introduced me to the problem and provided me with data and invaluable insight during this year.

I also would like to thank my fellow students in the study hall for the numerous discussions and a positive atmosphere throughout this hectic period.

Finally, I would like to thank my family, friends, and my partner for all their unconditional support.

Runar Skorge Stranden

Bergen, 01.06.23

Abstract

In 2022 the electricity prices and grid tariffs were never higher, and industrial companies are seeking opportunities to lower their electricity bills. Today, the industry is subject to three charges: A monthly fixed charge, a demand charge to the grid operator, and a cost per kilowatt-hour. The market determines the price per kilowatt-hour, and the peak demand charge is billed monthly for the highest peak power bought from the market. One option for lowering electricity costs is installing Photovoltaic (PV) systems to produce electricity for consumption and selling to the grid. With falling battery prices, new opportunities arise, and the industry is questioning if such energy storage investment can be a good idea for their facility. This thesis analyzes how optimally operated batteries, combined with PV systems, can lower the cost of electricity for industrial facilities. The demand for electricity and power production is uncertain, and, therefore, we develop a scenario-based multistage stochastic optimization approach to answer this question. Our study shows that an approach considering uncertainty can lower the cost substantively compared with the deterministic approach. This study emphasizes that it is essential to consider load and production as uncertain variables to grasp how much such installations can reduce electricity costs.

Contents

List of Figures

List of Tables

Abbreviations

ALM Augmented Lagrangian Method

B&B Branch-and-Bound

EVPI Expected Value of Perfect Information

IEA International Energy Agency

kWh kilowatt-hour

kWp kilowatt-peak

LP Linear Programming

MILP Mixed-Integer Linear Programming

PHA Progressive Hedging Algorithm

PV Photovoltaic

PVGIS Photovoltaic Geographical Information System

QRF Quantile Regression Forest

SARAH Solar Surface Radiation Data Set - Heliosat

VSS Value of Stochastic Solution

1 Introduction

1.1 Motivation

The Norwegian transmission system operator, Statnett, has issued that a substantial part of the grid has capacity issues and needs room for more power-demanding industries [1]. The grid is getting upgraded, but these expansions have significant investment costs and involve a bureaucratic process that takes time [2].

The Norwegian Water Resources and Energy Directorate writes in their report [3] that to ensure power balance in the Nordic grid by 2030, more of the electricity demand must be flexible.

As a consequence, not only must the industry pay a peak demand charge, but as of 2022, private households must also pay for their highest peak bought from the grid [4]. A peak demand charge encourages consumers to flatten out their consumption by lowering their electricity usage or moving the flexible part of the demand. Private households may be able to change the time they charge their car and wash their clothes, but this is often more complicated in the industry, where shifting electricity demand might be expensive. For instance, it might be necessary to maintain a warm temperature in the office buildings, provide energy to vessels at the dock or run the crushing mill.

When the demand is not flexible, installing additional energy storage, such as a battery, might be necessary to lower the peak demand and the electricity bill.

Whether a Photovoltaic (PV) system is a good investment highly depends on the spot price. In 2022 Europe was in an energy crisis. We have seen record-high spot prices multiple times, and the future market indicates that the situation will last even longer. And in Norway, in the industry sector, the subsidizing of electricity costs is limited compared to private households.

Falling prices for PV systems and rising spot prices make PV systems a better investment for lowering demand for electricity from the energy market and is therefore gaining significant attention in Norway [5]. But the sun does not necessarily shine when there is power demand, and the industry is questioning if battery storage is a smart investment when installing a PV system.

Record-breaking spot prices are just one of our concerns in the future energy market. Hydropower has provided Norwegian consumers with renewable energy for decades. Being reliable and cheap is one of many advantages. Hydropower is also flexible and has the ability to store

potential energy in reservoirs for periods of high demand. These storage capabilities can be a shock absorber and have helpt keep the spot prices reasonable [6]. The green transition leads to vast electrification and decarbonization, and we see a substantial increase in demand for renewable energy. International Energy Agency (IEA) forecasts that renewable energy will surpass coal as the largest source of electricity in 2025 [7].

With most potential hydropower plants already developed, new renewable power plants mainly generate electricity from intermittent sources, with solar and wind being the largest contributors. And according to the studies [8] and [9], increasing the share of the electricity generated from intermittent sources can increase the volatility of the spot price.

A battery can reduce electricity costs for an industrial facility in multiple ways. The battery can store power generated from PV systems when the production exceeds the electricity demand on the site, avoiding selling the power at a potentially lower cost.

A battery can also take advantage of the volatile spot prices by charging when the price is low and discharging when the price is sufficiently high. We call this operation *price arbitrage* operation. Also, supplying the load from the battery when there is high demand can reduce the peak demand charge. This operation is called *peak shaving*. An optimally operated battery takes advantage of low spot prices without increasing the peak load charge too much. This can be challenging since electricity demand, power generated from a PV system, and the spot price all have an uncertain nature.

1.2 Problem statement

During the energy crisis in 2022, the industry sector in Norway faced substantial electricity bills and has since sought opportunities to lower this expense. Investing in PV systems is gaining significant attention, and a question frequently being asked is if battery storage combines well with intermittent energy resources. These investments can be hard to evaluate since a battery can lower the bill both by peak demand reduction and by price arbitrage. And the stochastic nature of electricity demand, solar radiation, and electricity prices complicates this further.

We aim to evaluate these decisions such that the industry can understand the potential benefits and downsides of such an investment. By not addressing all the potential economic upsides with such an investment, the investment can get avoided, and the grid operators lose much-needed flexibility. Overvaluing such an investment, for instance, by ignoring uncertainty, can lead to a disappointed purchaser.

The type of installations we will investigate is illustrated in Figure 1. This thesis analyzes how

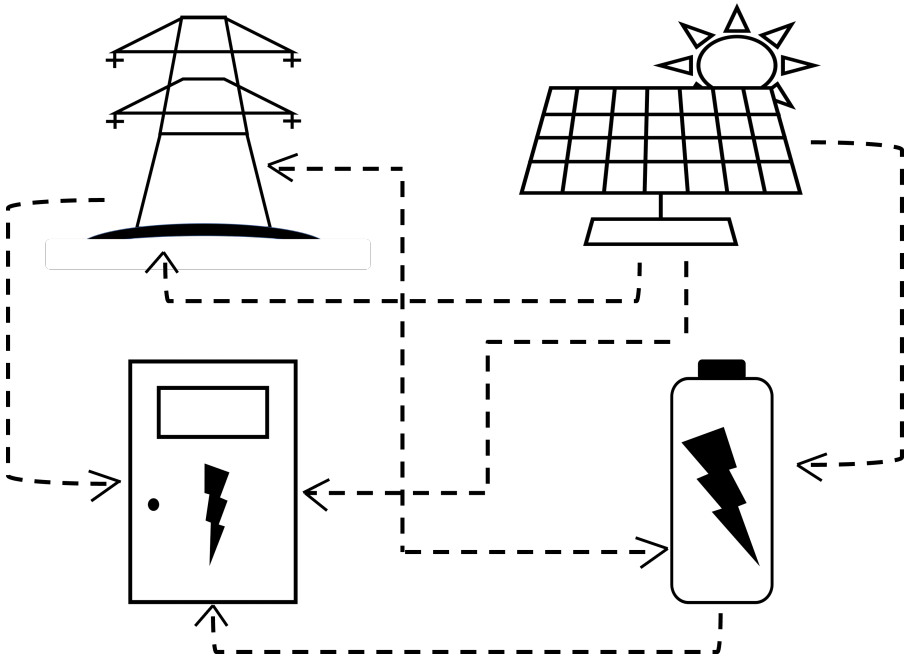

Figure 1: Power system with grid (top left), PV system (top right), load (bottom left), and battery (bottom right). An electrical connection is illustrated with dashed lines.

combining the PV system and optimally operated battery storage can lower electricity costs. Specifically, we will address the following research questions:

- How can an optimally operated battery reduce electricity costs?
- Is it reasonable to assume perfect information about the uncertain variables when evaluating how much batteries can reduce costs?
- How does a stochastic approach perform compared to a simpler deterministic method?

To answer these research questions, we first develop a deterministic model and then expand it to a multistage stochastic optimization model to better address uncertainties. Because of how the peak demand charge is calculated, we limit this study to industrial facilities.

By researching these questions, we aim to understand better the utilization of batteries for cost reduction.

1.3 Thesis overview

This thesis starts with an introduction to the topic of this study. The rest of the thesis is organized as follows:

- Chapter 2 provides the fundamental theory in optimization, a literature review, and proposes the approach this study takes.
- Chapter 3 describes the mathematical models, scenario generation method, and the data.
- Chapter 4 presents the results from the mathematical models.
- Chapter 5 concludes this study along with suggestions for future work.

2 Background

This chapter presents the fundamental theory of this study, including deterministic and stochastic optimization. Subsequently, we conduct a literature review providing oversight over similar work on optimizing battery operation for electricity cost reduction.

2.1 Theory

2.1.1 Deterministic modeling

G. B. Dantzig was the first to put Linear Programming (LP) in wide use during the Second World War, and it has since been applied for solving optimization problems [10]. The algorithm utilizes linear objective functions and constraints to solve problems where the objective is to maximize or minimize the function subject to a set of constraints. A feasible region defined by linear constraints is called a *polyhedron* [11].

For solving an optimization problem, each decision variable is assigned a value that satisfies all constraints while optimizing the objective function. A set of values that satisfies the constraints is called a feasible solution.

A LP problem can be formulated as

$$\text{maximize} \quad \sum_{j=1}^{n} c_j^{\mathsf{T}} x_j \tag{1}$$

$$\text{subject to} \sum_{j=1}^{n} a_{ij} x_j \leq b_i \quad i = 1, 2, ..., m \tag{2}$$

$$x_j \geq 0 \quad j = 1, 2, ..., n. \tag{3}$$

Where Equation (1) is the objective function and Equations (2) - (3) are constraints.

The simplex method was also introduced during the late 1940s and is a well-established algorithm for solving LP problems [10]. The algorithm finds the optimal solution by iterating through the polyhedron's vertices while improving the objective function value. The algorithm terminates when no neighboring vertex has a better solution or when determining that the problem is infeasible or *unbounded*. A problem is unbounded when the objective function value can be arbitrarily large without violating constraints.

The algorithm running time depends on the problem's size and is not guaranteed to be polynomial. However, the simplex method works very well in practice and is still used even for LP

problems of considerable size.

Consider the LP problem

$$\begin{aligned} \text{maximize} \quad & 3x_1 + 5x_2 && (4)\\ \text{subject to} \quad & x_1 + 2x_2 \leq 4 && (5)\\ & 2x_1 + x_2 \leq 6 && (6)\\ & x_1, x_2 \geq 0. && (7) \end{aligned}$$

The first step of the simplex method is to add *slack variables* and a variable ξ representing the objective function

$$\begin{aligned} \zeta &= \sum_{j=1}^{n} c_j^{\mathsf{T}} x_j \\ s_i &= b_i - \sum_{j=1}^{n} a_{ij} x_j \quad i = 1, 2, ..., m. \end{aligned}$$

Then the problem can be expressed in standard form,

$$\begin{aligned} \zeta &= 3x_1 + 5x_2 \\ s_1 &= 4 - x_1 - 2x_2 \\ s_2 &= 6 - 2x_1 - x_2 \\ x_1, x_2, s_1, s_2 &\geq 0. \end{aligned}$$

This is the initial *dictionary*. As it progresses, the algorithm iterates through dictionaries to search for the optimal solution. Each dictionary consists of m *basic* variables and n *non-basic* variables, with $\mathcal{B}$ representing the collection of indices corresponding to the basic variables and $\mathcal{N}$ denoting its complement[12].

At the start, we choose which variables that will be considered basic and which will be considered non-basic. For the LP problem we discussed earlier, x_1, x_2, s_1, and s_2 are the variables. Since the algorithm works by iterating through vertices, we need a feasible starting point. As mentioned in [12], this is not always straightforward, but in this example, we see that the problem is feasible in the origin.

Variables x_1 and x_2 are chosen as the non-basic variables, and s_1 and s_2 as the basic. This starting point corresponds to the feasible solution in which $x_1 = x_2 = 0$ and $s_1 = 4$, and $s_2 = 6$.

In the next iteration of the simplex method, one of the non-basic variables is selected to become basic, and one of the basic variables is selected to become non-basic. Choosing which variables to switch depends on improving the objective value and the problem's constraints.

The entering variable is chosen from the set of non-basic variables by the rule pick k from $\{j \in \mathcal{N} : c_j > 0\}$. The leaving variable is chosen from the set of basic variables by the rule pick l from $\{i \in \mathcal{B} : \frac{a_{ik}}{b_i}$ is maximal$\}$. If there is no non-negative ratio in the column, the problem is unbounded.

The solution is optimal if all the coefficients in the objective function's row are non-negative. If a negative coefficient exists, we can improve the solution by another iteration.

The problem we have discussed can be solved as follows:

1. Select the entering variable: Since $c_1 = 3 > 0$ and $c_2 = 5 > 0$, we have two choices for the entering variable and select the lowest value, x_2.

2. Select the leaving variable: We calculate the ratio between the constraint's coefficient of x_2 and its right-hand side: $\frac{a_{12}}{b_1} = \frac{2}{4} = 0.5$, $\frac{a_{22}}{b_2} = \frac{1}{6} = 0.167$. Since $\frac{a_{12}}{b_1}$ is larger than $\frac{a_{22}}{b_2}$, we choose $x_1 + 2x_2 \leq 4$ as the constraint to pivot on and s_1 as the leaving variable.

3. Update the dictionary: We perform the pivot operation by updating the values of x_2, s_1, and the right-hand side of the constraints. We calculate the new value of x_2 by solving for it in terms of x_1 and s_1: $x_2 = \frac{4-x_1}{2}$ We then update the values of s_1 and the right-hand-side of the constraints: $s_1 = 4 - x_1$, right-hand side $= [0, 4 - x_1, 6]$.

4. Repeat steps 1-3 until an optimal solution is found or until it is determined that no optimal solution exists.

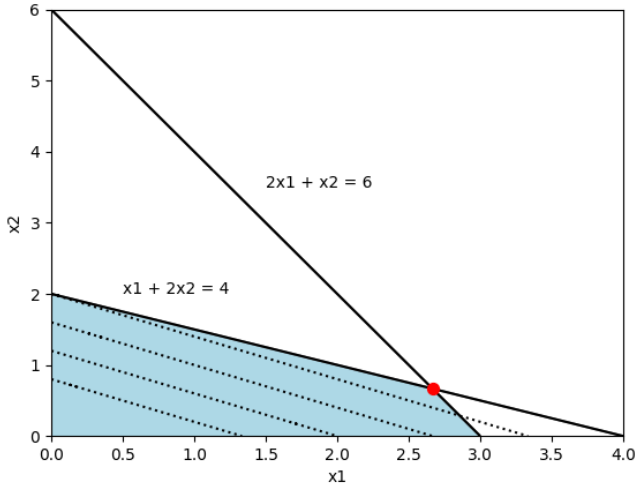

Figure 2: Feasible region and level curve for LP problem

After a few iterations, the algorithm finds the global optimum at the vertex indicated by the red dot in Figure 2. We confirm that this is the optimal solution by plotting the level curve of

the objective function and seeing which of the vertices it reaches the last.

But what if we add the constraint

$$x_1, x_2 \in \mathbb{Z}, \tag{8}$$

requiring that all the decision variables must be integer valued? This problem now becomes a form of a Mixed-Integer Linear Programming (MILP) problem. Figure 3 shows that the optimal solution of a MILP problem may not be located at a vertex of the feasible region. The simplex method is not guaranteed to find the optimal solution for MILP problems since the algorithm only checks solutions in the vertices, and the feasible region of a MILP is limited to a set of points and not a continuous polyhedron. The only time the algorithm is guaranteed to find the global optimal solution of such a problem is when each vertex is represented by integers only.

If this is true, the constraints form the *convex hull*, where convex is a property of a set of points, which means any line segment joining any two points in the set lies within the set [13]. The convex hull is the smallest convex set that contains the feasible region of the MILP problem [11].

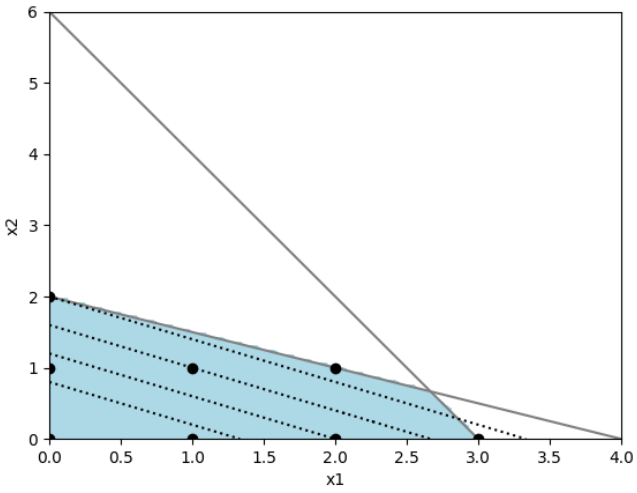

Figure 3: Feasible region and level curve for MILP problem

When dealing with MILP problems, finding the optimal solution can be much more challenging. The feasible region is restricted to integer values, and there is no guarantee that the polyhedron represents the convex hull. As described in [11], a given two formulations P_1 and P_2, P_1 is a better formulation of the feasible area if $P_1 \subset P_2$. We, therefore, need algorithms for reducing the size of the formulations of the problem.

There has been produced a wealth of literature facing these problems, and Ralph E. Gomory introduced a cutting plane algorithm in 1958 [14]. And this was later expanded to the Branch-and-Bound (B&B) method [15]. The method works by breaking the problem into a series of smaller problems. We refer to these new problems as *subproblems*.

The steps of the B&B algorithm are

1. Start with an initial relaxation of the problem, where the integer constraints on the variables are ignored. Solve this relaxed problem to obtain the optimal objective function value and the corresponding optimal solution.
2. Choose one of the integer variables with a fractional value and create two subproblems by adding constraints that restrict the variable to be either less than or equal to or greater than or equal to its integer part.
3. Solve each subproblem and obtain the optimal objective function values and solutions.
4. Keep track of the best feasible solution found so far.
5. Discard subproblems that cannot possibly contain a better feasible solution than the currently best solution. The algorithm terminates when all paths are explored.

The enumeration tree for solving the integer optimization problem described by equations (4)-(7) and (8) is shown in Figure 4.

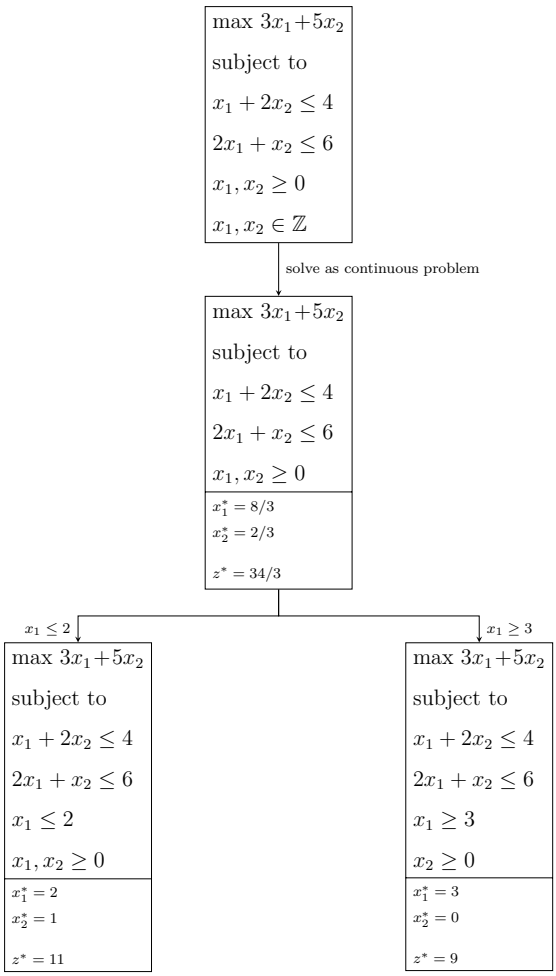

Figure 4: Branch-and-Bound method

The problem in Figure 4 is relatively small and can be solved quickly with only one branching, but solving larger integer optimization problems can be challenging. For instance, the B&B algorithm is sensitive to which order the subproblems are solved, so inefficient branching can significantly increase the solution time.

Solving MILP problems are generally challenging, and as mentioned in [16], the industry often accepts solutions significantly away from the optimal since the computation time of these algorithms can be immense. As a consequence, techniques for solving such problems approximately is developed.

A *heuristic* algorithm is designed to find an approximate solution to a problem more quickly when classic methods are too slow or fail to find any exact solution and are often used to solve complex optimization problems that involve large, nonlinear, non-convex, or stochastic models [17].

In summary, it is essential to set realistic expectations for both the solution time and quality

of any optimization algorithm when solving MILP problems.

LP and MILP problems are both parts of deterministic optimization. A weakness of these approaches is that they are generally unable to produce optimal solutions when dealing with uncertain formulations. The next section introduces stochastic optimization.

2.1.2 Stochastic modeling

While optimization methods that rely on deterministic assumptions may not be effective when facing uncertainty, stochastic optimization aims to find solutions close to optimal, even when dealing with random data. Stochastic optimization is also known as *optimization under uncertainty*. Using probabilistic assumptions, we can consider the uncertainty of the problems and find solutions that are more likely to succeed in various scenarios [18].

Stochastic problems are often formulated in two stages. In the first stage, a decision must be made before important information is known [19]. Then, the uncertainty is revealed in the second stage, and a second decision is made. This second decision is called a *recourse* decision. This action is made to minimize or maximize the objective function value based on the first stage decision and the revealed uncertainty.

Suppose that we can model the uncertainties of a problem as random variables ξ with a specific probability distribution. Then a two-stage optimization problem can be formulated as

$$\begin{aligned} &\min c^{\mathsf{T}}x + \mathbb{E}_{\xi}[Q(x,\xi)] \\ &\text{s.t } Ax = b \\ &x \geq 0, \end{aligned}$$

where x denotes the initial decisions made in the first stage, $Q(x,\xi)$ is the second-stage cost function that depends on both the initial decisions and ξ. The expectation is taken with respect to the probability distribution of ξ. This second stage cost function can be expressed as an optimization problem itself as

$$\begin{aligned} &Q(x,\xi) = \min q(\xi)^{\mathsf{T}}y \\ &\text{s.t } T(\xi)x + W(\xi)y = h(\xi) \\ &y \geq 0. \end{aligned}$$

The vector y represents the recourse variables, T is called the *technology matrix*, W is the *recourse matrix*, and h denotes the right-hand side of the constraints, all depending on the realization of the uncertain variables.

For a simple numerical example, we investigate the following problem:

$$\min \quad 2x + E_\xi[Q(x,\xi)] \tag{9}$$

$$x \geq 0 \tag{10}$$

where,

$$Q(x,\xi) = \min \quad 3y \tag{11}$$

$$\text{s.t. } x + y \geq \xi \tag{12}$$

$$y \geq 0. \tag{13}$$

In this two-stage stochastic problem, x is determined before the realization of the uncertainty, and then once ξ is realized, y is determined. Here the objective is to choose x to minimize the objective function value. This involves a trade-off since choosing x too small might incur an additional cost in the second stage.

While two-stage modeling can be valuable, many practical decision problems involve multiple decisions depending on the outcomes of previous decisions. Leading to the concept of multistage stochastic programs [18]. In this approach, decisions are made at each stage based on the information available, including previous decisions and the realizations of random variables. A multistage stochastic optimization problem can be formulated as of [20]:

$$Q_t(x_{t-1}, \xi_t) = \min_{x_t \in X_t} c_t^\mathsf{T} x_t + \mathbb{E}[Q_{t+1}(x_t, \xi_{t+1}) \mid \xi_t]$$

$$\text{s.t } W_t x_t = h_t - T_t x_{t-1}$$

$$\text{where } \xi_t = \{c_t, W_t, h_t, T_t\}.$$

Here the determination of x_1 is based on ξ_1, then after receiving the outcome ξ_2 makes a new decision x_2, taking into account both x_1 and the realizations of ξ_1 and ξ_2. The decision x_t depends on all ξ_i and x_i for all $i \in \{0, 1, ..., t-1\}$.

A challenge of stochastic optimization is how to model uncertain variables. The following section discusses how uncertainties of stochastic optimization problems can be represented in *scenario trees*.

2.1.3 Modeling uncertainty in terms of a scenario tree

Stochastic optimization is all about considering various outcomes of the uncertain variables ξ. A challenge is that ξ can be represented by a continuous probability distribution that the solution method cannot handle. We, therefore, need to approximate the distribution by discretization. This discretization is referred to as a scenario tree, where a *scenario* represents a possible outcome of the uncertain variables as a function of time [21].

Figure 5 illustrates a scenario tree. The tree divides into branches at the root node representing possible outcomes of the uncertain variable and that a decision under uncertainty must be made. A child represents a possible outcome, and each path from the root node to a leaf represents a scenario. In this tree, a decision is only made at the root node, making the problem two-stage.

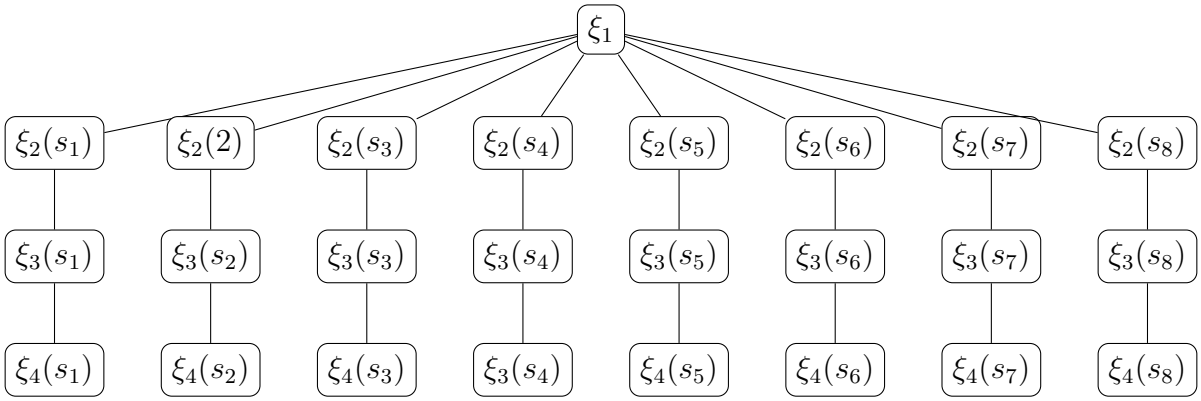

Figure 5: Two-stage scenario tree

On the other hand, a multistage scenario tree consists of multiple stages, where each stage is a moment in time when a decision is taken. Such a tree is more flexible, making it possible to model problems where effects carry over from one stage to another. For managing multistage scenario trees, we introduce some notation.

Let $\mathcal{S}$ be a finite set where each $s \in \mathcal{S}$ represents the scenarios. Denote by $\xi_t(s)$ be the outcome of the uncertain parameters revealed at t given that scenario s is realized. If $\xi_k(s_1) = \xi_k(s_2) \quad \forall k = 1, .., t$, we say that s_1 and s_2 are t-equivalent. Let Ω_t be the set of equivalence classes in the equivalent relation. Hence, a set $\omega \in \Omega_t$ consists of scenarios that coincide in all periods up to t, and all $s' \notin \omega$ differs from each $s \in \omega$ in at least one period $k \leq t$.

Looking at the scenario formulation of a stochastic problem as [20]:

$$\min \sum_{s\in\mathcal{S}} \sum_{t\in\mathcal{T}} p_s(c_{t,s}^{\mathsf{T}} x_{t,s}) \tag{14}$$

$$\text{s.t } W_{1,s}x_{1,s} = h_{1,s}, \quad \forall s \in \mathcal{S} \tag{15}$$

$$W_{t,s}x_{t,s} + T_{t-1,s}x_{t-1,s} = h_{t,s} \quad \forall s \in \mathcal{S}, t \in \mathcal{T} \setminus \{1\} \tag{16}$$

$$x_{k,s_1} = x_{k,s_2}, \quad \forall s_1, s_2 \in \omega, \forall \omega \in \Omega_t, \forall k \in \{1, ..., t\} \tag{17}$$

$$x_{t,s} \geq 0 \quad \forall s \in \mathcal{S}, \forall t \in \mathcal{T}. \tag{18}$$

Here, p_s denotes the probability of scenario s of occurring, and for a given stage t, scenarios with an equivalent relation up to t are grouped into the same partition $\omega \subset \mathcal{S}$. The set Ω_t represents the set of all ω induced by the equivalence relation up to t.

The *nonanticipativity constraint* (17) ensures that decisions at a given stage are identical for all scenarios that are t-equivalent, thereby ensuring that the decision is based only on available information and is not anticipating what will happen in the future [19].

In Figure 6, a 4-stage scenario tree is illustrated. In the following figure and similar figures in this thesis, the notation $\xi_t(s)$ is replaced with $\xi_t(\omega)$ to illustrate that for all $s \in \omega_i$ the same uncertainty is unrevealed.

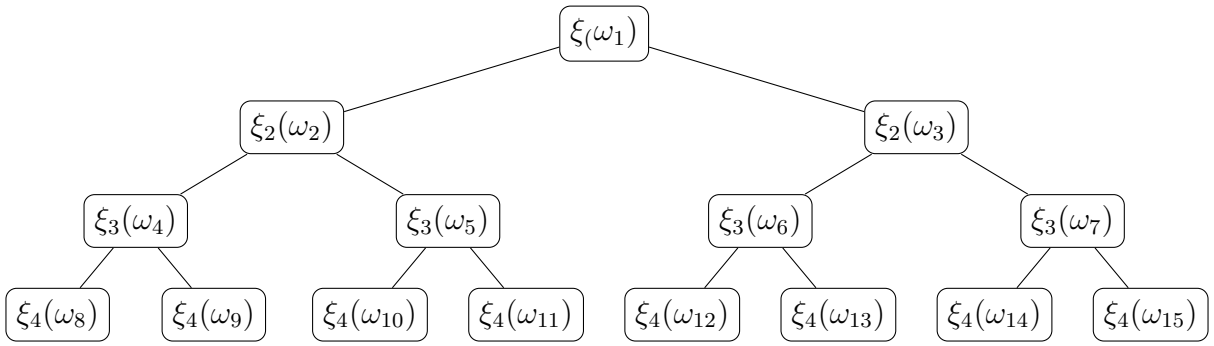

Figure 6: Multistage scenario tree

The process of constructing a scenario tree is called *scenario generation*. There has been developed a variety of algorithms for generation scenarios, including sampling, moment-matching, and path-based methods [21].

A suitable scenario generation method can discretize the stochastic process such that it is not the generation method that drives the problem but the model [19]. At the same time, the tree must be kept tractable. Hence, the critical issue of scenario trees is that they must adequately

represent the stochastic process underlying distribution, but with few enough scenarios such that the problem can be solved in reasonable time [22].

2.1.4 Progressive Hedging Algorithm

The Progressive Hedging Algorithm (PHA) was first presented by Rockafellar and Wets in [23] and is a popular method for solving stochastic optimization problems. It is used in various applications, including energy systems [24].

A challenge with stochastic problems is that they can get huge with the number of scenarios. The PHA handles this issue by breaking down the large problem into smaller subproblems by relaxing the nonanticipativity constraints. Now each scenario can be solved separately as a subproblem. Then, the algorithm iteratively solves the subproblems and achieves consensus on the nonanticipative constraints by penalizing the distance from the expected solution, $\bar{x}$.

The guarantee that the PHA converges to the global optimum relies on the assumption of the problem being convex. Despite this, the algorithm can still give valuable results as a heuristic, for instance, in MILP problems [25].

PHA is based on the *Augmented Lagrangian Method (ALM)* [26]. With the ALM, an optimization problem, such as

$$\begin{aligned} &\min f(x) \\ \text{s.t } &g_1(x) = 0 \\ &g_2(x) = 0 \\ &x \geq 0, \end{aligned}$$

is relaxed by inserting the constraint in the objective function using a penalty function. Resulting in

$$\begin{aligned} &\min f(x) + \rho\psi(g_1(x)) \\ \text{s.t. } &g_2(x) = 0 \\ &x \geq 0, \end{aligned}$$

where ρ is a positive penalty parameter and ψ is a penalty function. Applying ALM on (14) - (18) gives the Lagrangian function

$$L(x, \bar{x}, y, \lambda) = \sum_{s \in \mathcal{S}} \sum_{t \in \mathcal{T}} p_{t,s}(c^{\mathsf{T}} x_{t,s} + \lambda_{t,s}^{\mathsf{T}}(x_{t,s} - \bar{x}_{t,\omega}) + \frac{\rho}{2}||x_{t,s} - \bar{x}_{t,\omega}||^2).$$

The final term in the equation, represented by ψ, is a quadratic function that serves as a penalty function. Despite the connected nature of all scenarios through $\bar{x}$, the problem can still be solved through an iterative approach. This approach entails replacing $\bar{x}$ with its updated estimate $\bar{x}^{(k+1)}$ from the preceding iteration, which is typically calculated as the expected value:

$$\bar{x}_{t,\omega} = \sum_{s \in \omega} \frac{p_s x_{s,t}}{\sum_{s \in \omega} p_s}.$$

The update of the Lagrange multipliers then becomes

$$\lambda_{t,s}^{(k+1)} = \lambda_{t,s}^{(k)} + \rho^{(k)}(x_{t,s}^{(k+1)} - \bar{x}_{t,\omega}^{(k+1)}),$$

which then leads to the Lagrangian function

$$L(x, \lambda) = \sum_{s \in \mathcal{S}} \sum_{t \in \mathcal{T}} p_s(c_{t,s}^{\mathsf{T}} x_{t,s}) + (\lambda_{t,s}^{(k)})^{\mathsf{T}}(x_{t,s} - \bar{x}_{t,\omega}^{(k)}) + \frac{\rho^{(k)}}{2}||x_{t,s} - \bar{x}_{t,\omega}||_2^2).$$

The solution is considered to have converged when it is sufficiently close to $\bar{x}_{t,\omega}$. The convergence criterion is defined as:

$$\delta^{(k)} = \sum_{s \in \mathcal{S}} \sum_{t \in \mathcal{T}} p_s ||x_{t,s}^{(k)} - \bar{x}_{t,\omega}^{(k)}||.$$

The complete algorithm is presented in Algorithm 1.

The penalty parameter ρ plays a crucial role in the PHA. In the original work of Rockefeller and Wets, it was pointed out that the algorithm is guaranteed to converge to an optimal solution, for any $\rho > 0$, given that the problem is convex [23]. But they did not provide any guidance on how to choose it.

Mulvey and Vladimirov [27] later pointed out that the algorithm is sensitive to this parameter and that a high value of ρ typically converges faster but to a suboptimal solution. In contrast, low values yield weaker enforcement of the nonanticipativity constraints and result in a more gradual convergence to close to optimality, but after many iterations.

As discussed by Zehtabian and Bastin [28], various strategies have been proposed for setting the penalty parameter, including dynamic updates. For instance, the method presented by Zéphyr et al. [29] updates the parameter based on the nonanticipativity and optimality gap. Hvattum and Løkketangen [30] proposed a method that investigates dual and primal convergence, and Goncalves et al. [31] suggested an approach where the parameter starts at a low value and gradually increases.

Despite these many strategies, there is still no consensus on the optimal approach for initializing the penalty parameter in the PHA.

2.2 A literature review on the utilization of batteries for electricity cost reduction

Batteries for cost reduction either by peak demand charge reduction, price arbitrage, or both has produced a wealth of literature in recent years. This section aims to provide an overview of the existing literature in the field and how it addresses these issues.

2.2.1 Peak shaving

Peak shaving is a technique used to reduce electricity consumption during periods of maximum demand. It works as follows with a battery:

- Charge the battery: During low demand, the battery charges up by storing the excess power. This is typically during off-peak hours, like late at night.
- Discharge the battery: During peak times, when demand is high, the battery discharges its stored power to reduce the amount of power bought from the grid.

Peak shaving aims to minimize the costs associated with peak electricity demand. These peak times incur demand charges, which are additional fees based on your highest rate of energy usage during a billing cycle. Over which periods these peaks are calculated and also the billing cycles are defined varies. In [32–34] the billing cycle was monthly, and the demand charge was based on a single maximum demand over a 15-minute period. While the Norwegian case study [35] utilized a monthly billing cycle with the highest hourly consumption during a month as the peak demand.

Various papers have explored the opportunity to utilize a battery solely for peak shaving. In 2007, Oudalov et al. [32] presented a dynamic programming approach for reducing peak demand. An example of a large industrial customer was used to demonstrate the application of their methodology. The results indicated that, compared to a situation without a battery, there could be a potential reduction in the electricity bill by 4 %.

Later in 2014, Hanna et. al. utilized a linear optimization model for planning an energy dispatch schedule inside a 24-hour window using forecasts for electricity demand and solar power production [36]. They underscored the importance of accurate forecasts since only one single error inside the billing cycle can erase a large portion of the potential demand charge reduction.

The year after, Neumann and Simpson [33] studied the economic benefits of combining batteries

with PV systems for peak demand charge reduction by utilizing the National Renewable Energy Laboratory's Battery Lifetime Analysis and Simulation Tool [37].

This research responded to increasing mandates and incentives for energy storage in the USA with ambitious targets for energy storage by 2020. As part of these incentives, customers were encouraged to adopt batteries to reduce demand charges.

Interesting findings in this report are that the size of the PV system did not impact whether a battery is a good investment since the majority of the economic benefits come from peak shaving, and PV systems are generally unable to reduce the peak demand. They explained this by solar power production being intermittent and cannot produce stable enough over a long period of time. This is sensible since the demand charge is based on a single maximum over a 15-minute period in a monthly billing cycle.

Another finding in this report, which is supported by [36], is that the shape of the electricity demand profile is vital when considering the benefits of installing a battery for peak shaving applications. The reason for this is that a high peak over a short period requires a relatively low amount of energy compared to a more uniform case where the peaks last over longer periods. In their discussion, they point out that the amount of energy needed increases nonlinearly with the peak reduction amount.

The work done by Oudalov et al. [32], Hanna et al. [36], and Neumann and Simpson [33] gives interesting insights into the potential of peak demand charge reduction with battery. However, they share a common limitation of relying on deterministic assumptions of electricity demand and solar power generation. Possessing perfect information about the future is unrealistic, and the potential cost reduction can be exaggerated in [32] and [37]. In the paper by Hanna et al., they assume a deterministic forecast, which can affect the potential cost reduction. A stochastic approach might be more robust to uncertainties in the forecast. Additionally, their focus is exclusively on peak shaving applications and does not consider the potential advantages of price arbitrage. The next section of the literature review focus on studies investigating utilizing batteries for price arbitrage operations.

2.2.2 Price arbitrage

Price arbitrage in energy markets refers to taking advantage of fluctuating electricity prices throughout the day to buy low and sell or consume when the price is high. It works as follows with a battery:

- Charge the battery: When electricity prices are low, the battery charges with energy from the grid.
- Discharge the battery: When electricity prices are high, typically during the late afternoon or early evening, the battery discharges its stored power back to the grid or is used to cover the electricity demand of the facility.

The fundamental principle here is buying power when it's cheap and spending or selling it when it's expensive.

Utilizing batteries for price arbitrage alone has been discussed in various papers. Youn and Cho [38] present a linear programming technique for combining a battery with a small power-producing facility to make it possible to buy and sell under the spot prices to the power grid. In 2015, Telaretti et. al. [39] investigated how to maximize the profit for the electricity customer by doing price arbitrage with a battery. They focused on testing various batteries for this application and the importance of accurate electricity demand forecasts. They utilized an operation strategy that works regardless of the shape of the facility's demand.

It is not only the spot price that is dynamically priced. Hassan et. al. [40] formulate a MILP problem for maximizing revenue from a PV system combined with battery storage under varying tariffs. They consider four different tariff structures in the UK where the price per kilowatt-hour (kWh) varies through the day. They also consider a feed-in tariff that makes it favorable to consume the energy instead of selling it to the grid.

While the studies reviewed consider various approaches to price arbitrage under different pricing structures, the consensus is that deploying batteries solely for price arbitrage operations is not economically viable in the long run. Therefore, much of the literature investigates both peak demand and price arbitrage.

2.2.3 Combined peak shaving and price arbitrage

In 2019, Berglund et al. [35] presented a MILP model that minimized the electricity bill by considering both the peak demand charge and the spot price while considering battery degradation.

Operating a battery causes degradation at some level. Frequently charging and discharging a battery on a high level can cause high temperatures and accelerate degradation, leading to shorter battery life. It can therefore be an important aspect to consider in the modeling since

replacing batteries is expensive.

They ran a year-long, hourly resolution simulation based on the 2018 spot prices. Their battery degradation model resulted in the battery charging and discharging only a relatively small amount of energy each time. Interestingly, no energy was sold to the grid during this period, and peak shaving was the most significant contributor to the reduction in the electricity bill. When they conducted a sensitivity analysis on the spot prices, it revealed that spot price volatility led to more active battery operation and, consequently, greater earnings.

Schneider et al. [41] also consider a MILP formulation of the problem. They investigate both peak shaving and price arbitrage while accounting for battery degradation. The simulation of a Swiss facility shows that 95.6 % of the cost reduction was because of peak shaving and only an additional 4.4% was achieved by price arbitrage operations. Other findings from the study are that in that case, the trade-off between peak shaving and price arbitrage is minimal, and similar to [36, 37], they illustrated that the amount of peak shaving is sensitive to the shape of the electricity demand profile.

2.2.4 Stochastic modelling

The papers discussed so far rely on deterministic assumptions. By assuming a perfect forecast, the estimated economic benefits of implementing a battery can be too high, and a deterministic forecast can make the algorithm sensitive to errors. With a stochastic approach, more realistic results can be obtained. In contrast to deterministic assumptions, a stochastic approach addresses uncertainty in the forecasts, making it more robust to forecast errors and providing a more realistic estimation of the benefits of battery storage systems.

Hafiz et al. [42] utilize a multistage stochastic optimization model and the Stochastic Dual Dynamic Programming Algorithm to address uncertainty in electricity demand and solar power production. Machine learning is used for forecasting and construction of the scenario tree. The case study results in an 8.4 % reduction in electricity costs compared to the scenario without battery storage. While the study provides exciting results and methodology, they do not consider peak demand charge or battery degradation.

In their study, "A Two-Stage Stochastic Programming Model for Energy Management in Local Electricity Systems with Peak Shaving Service," de la Nieta et al. formulate an approach to battery scheduling in southern Norway [43].

They introduce a two-stage stochastic MILP model to maximize the expected operating profit

based on peak shaving and price arbitrage. They integrated uncertain parameters, which were modeled using scenarios based on historical data that capture the stochastic nature of demand, PV generation, and spot prices. This study shows that peak shaving service and price arbitrage alone do not make battery systems under the current pricing and regulatory framework profitable. They also emphasize that the battery's efficiency is an important aspect to consider. While de la Nieta et al. give valuable insights into battery operation in a stochastic environment, their scenario generation procedure may not fully account for the uncertainties in the parameters. Also, incorporating more than two stages in the decision-making process can give a more flexible decision-making process. However, this comes with its own set of challenges, like an increased computational burden and the need for more detailed data.

2.2.5 Proposed approach

Based on the literature review, how to optimally operate a battery for electricity cost reduction has produced many research papers in recent years. Most studies rely on deterministic assumptions, while limited work has used multistage stochastic optimization considering both price arbitrage and peak shaving.

While we acknowledge that considering a realistic battery model with degradation will affect the results, the runtime of over one hour presented in [35] leads to disregarding battery degradation in this study. A stochastic formulation of the problem will be larger than a deterministic one, and the computational load must be kept low.

By identifying the gaps in the current literature, our study focuses on a multistage stochastic optimization problem, including price arbitrage and peak shaving applications.

To the best of the author's knowledge, the concepts of Value of Stochastic Solution (VSS) and Expected Value of Perfect Information (EVPI) are not discussed in this literature. By addressing these concepts, we aim to expand the understanding of optimally operated batteries considering uncertain electricity demand and solar power production.

3 Methodology

This chapter presents the methodology used in this study to explore how a battery can reduce electricity bills. In that context, we need data from different sources, including electricity prices, consumption, solar power production, and weather data.

Two different mathematical models are used. The deterministic model is presented before expanding to a multistage stochastic optimization model. The scenario generation method is vital for representing uncertainty in the stochastic approach and is also outlined.

Various metrics and the base case are presented to compare the results of the different approaches.

3.1 Data

3.1.1 Consumption

Smart electricity meters were implemented in Norway in 2018 and 2019. These meters can measure real-time information about voltage, current, and electric power. Because of privacy matters, only hourly consumption data is shared from the meter and stored in Elhub. Elhub is a comprehensive database that stores all electricity production and consumption data in Norway.

This study utilizes data from an office building that spans from January 2021 until the beginning of February 2023. The raw data obtained from Elhub requires cleaning and preprocessing before it is suitable for analysis.

3.1.2 Electricity prices

Understanding how the electricity bill for an industrial facility is put together is vital when utilizing a battery. This section describes the components of the electricity cost and discusses spot price levels and volatility.

The electricity price for an industrial facility is split into four parts:

1. The cost per kilowatt-hour bought from the grid.
2. The revenue from selling electricity production to the grid.
3. The peak demand charge.
4. A fixed fee to the grid operator.

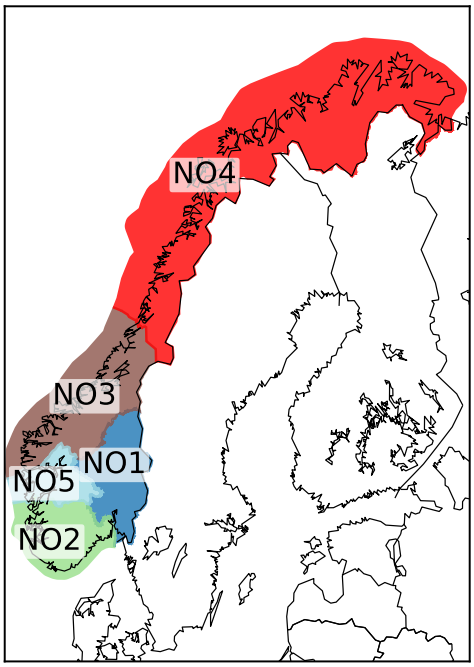

Figure 7: Nord Pool price areas

Since the fixed fee remains constant and does not affect the outcome of the analysis, it will not be discussed further. Buying kWh of electricity consists of four components: the spot price determined by the power market, Nord Pool. In addition to the energy tariff and consumption tax paid to the grid operator for the given location and the markup to the electricity provider. In this study, the electricity is bought from price area NO5, with Volte as the electricity provider and BKK as the grid operator. BKK and Volte have fixed prices for 2022, while the market determines Nord Pool's prices. The market prices for each hour are published daily at 13:00 for the following day.

The demand cost is calculated as the monthly peak demand multiplied by the demand tariff.

When electricity is sold back to Volte, the revenue is determined only by the spot price for the given hour, without including the energy tariff, consumption tax, or markup.

Table 1 shows the price per kWh for energy, peak load demand, and markup to the electricity provider.

Table 1: Peak demand tariffs, energy tariffs, consumption taxes, and markup [44] [45]

	Demand Tariff [NOK/kWh]	**Energy Tariff [NOK/kWh]**	**Consumption Tax [NOK/kWh]**	**Markup [NOK/kWh]**
Winter	59	0.07	0.0916	0.0198
Summer	49	0.06	0.1584	0.0198

Figure 8 illustrates the monthly average spot price from 2012. It shows a prediction up until 2026, provided by Eviny Fornybar. The figure shows that the prices were stable from 2012 before a drop in 2020 caused by the corona pandemic. Then, the Energy Crisis hit in 2021, causing record-high prices that peaked in August 2022. These trends can potentially explain why investing in PV systems has recently gained significant attention in Norway.

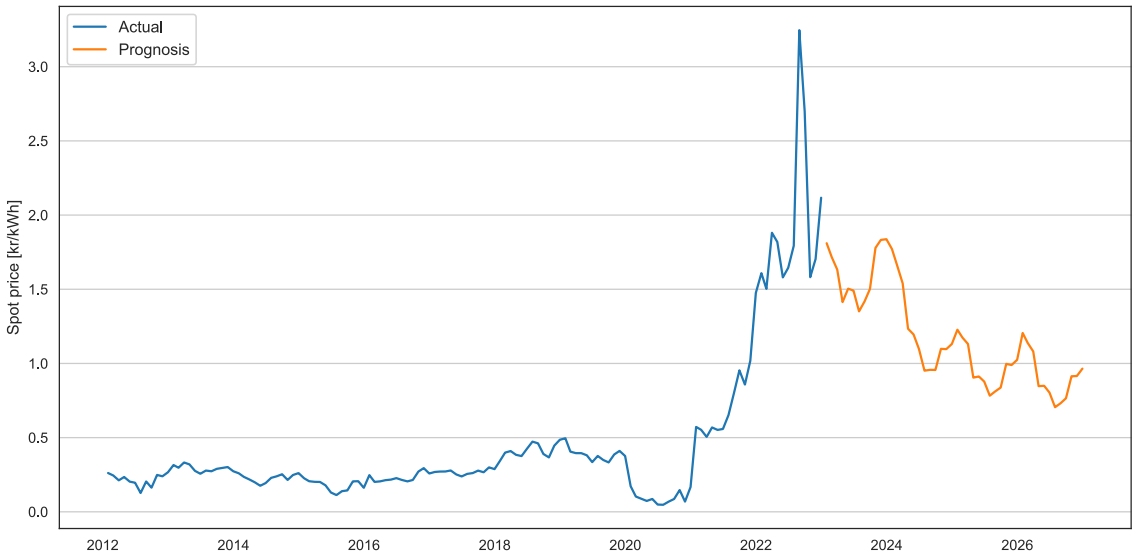

Figure 8: Monthly Average NO5 Spot Prices: Historical and Predicted Trends (2012-2026)

The daily fluctuations of the spot price are important for battery operations. This volatility enables price arbitrage operations, such that the battery can charge during cheap hours and discharge when expensive. For our study, we interpret volatility as the daily standard deviation σ of the spot price. This can be expressed as

$$\sigma = \sqrt{\frac{1}{23}\sum_{i=1}^{24}(x_i - \bar{x})^2} \tag{19}$$

where,

- x_i denotes the i^{th} spot price observation.
- $\bar{x}$ is the daily average spot price, calculated as $\frac{1}{24}\sum_{i=1}^{24} x_i$.

In this section, we've broken down the makeup of electricity prices, how they hit industrial facilities, and how they can guide battery operations. The understanding of these elements is fundamental to the following modeling and analysis.

3.1.3 Solar power generation

The solar power production data used in this study is obtained from the Photovoltaic Geographical Information System (PVGIS) using the Solar Surface Radiation Data Set - Heliosat (SARAH), which is a comprehensive resource offering solar radiation and temperature data for simulating photovoltaic systems [46]. To retrieve relevant data, we input the configurations of the PV systems we want to simulate, which include longitude, latitude, tilt, azimuth, energy loss factors, and the capacity of the PV system measured in kilowatt-peak (kWp).

Longitude and latitude determine the geographical location of the PV systems, while tilt and azimuth represent the panels' mounted angles relative to the roof and sky direction, respectively. Since some energy is lost during transmission through cabling and conversion by inverters, the production data is multiplied by a number less than one.

3.1.4 Weather data

This study utilizes weather data to predict electricity demand and solar power production. The data is from the weather station on Florida and is retrieved from The Norwegian Meteorological Institute [47].

We use historical temperature data for predicting electricity demand, while temperature and cloud cover data are utilized for predicting solar power production. Temperature data can be valuable for forecasting demand since heating and cooling have a major impact on consumption patterns for many facilities [48].

Cloud data is vital for predicting solar power generation since the amount of cloud cover explains the amount of solar radiation that will reach the panels. Combining temperature and cloud data provides a good foundation for forecasting solar power generation from a PV system [49].

3.2 Deterministic model

This study examines a system consisting of a battery (B), a PV system (E), the electric grid (G), and demand (D). The components and the connections are illustrated in Figure 9. The figure shows that the demand can draw energy from the battery, grid, and the PV system. The grid can receive power from both the battery and the PV system, and the PV system can serve the battery, the demand, and the grid. The battery can charge from the grid and PV system and discharge to the demand and the electric grid.

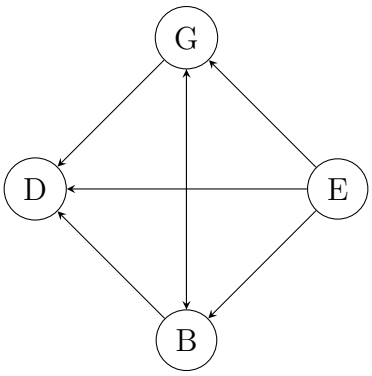

Figure 9: Schematic representation of the connections in the power system. Arrows indicate the possible energy transfer between components.

3.2.1 Decision variables and sets

This study aims to manage the *energy flows* in the connections to minimize cost. To do this we assign decision variables to the flows for each hour. The set $\mathcal{M}$ represent the set of months under consideration for the problem, and $\mathcal{T}_m$ represents the set of all hours in each month m.

Each arc in Figure 9 corresponds to a decision variable, such that

- The energy flow from the PV system in month m and hour t is represented by $x_{t,m}^{ED}$ for the demand, $x_{t,m}^{EB}$ for the battery, and $x_{t,m}^{EG}$ for the grid.
- The energy flow from the battery is denoted by $x_{t,m}^{BD}$ for the demand and $x_{t,m}^{BG}$ for the grid
- The energy flow from the grid to the battery and the demand are represented by $x_{t,m}^{GB}$ and $x_{t,m}^{GD}$, respectively.

In addition, the model consists of decision variables corresponding to the peak demand l_m, binary variables $\mu_{t,m}$ and $\pi_{t,m}$ and the battery $r_{t,m}$. They are addressed later in the section.

3.2.2 Constraints

To optimally operate a battery in this setting has certain limitations, and this section aims to define the feasible area of the problem and describe the constraints.

The battery is a vital model component represented by its energy content $r_{t,m}$. With the constraint

$$r_{t_0,m_0} = 0$$

where t_0, m_0 represents the first hour of the first month, we initialize the battery as empty. To ensure that the battery content does not exceed the capacity B, we impose the constraint

$$r_{t,m} \leq B \qquad \forall m \in \mathcal{M}, \forall t \in \mathcal{T}_m.$$

It is crucial to maintain energy balance and the equations

$$\begin{aligned} r_{t+1,m} &= r_{t,m} + x^{EB}_{t,m} + x^{GB}_{t,m} - x^{BD}_{t,m} && \forall t \in \mathcal{T}_m \setminus |\mathcal{T}_m|, \forall m \in \mathcal{M} \\ r_{1,m} &= r_{|\mathcal{T}_m|,m-1} + x^{EB}_{|\mathcal{T}_m|,m-1} + x^{GB}_{|\mathcal{T}_m|,m-1} - x^{BD}_{|\mathcal{T}_m|,m-1} - x^{BG}_{|\mathcal{T}_m|,m-1} && \forall m \in \mathcal{M}, \end{aligned}$$

ensure that the battery content at time t depends on the state and energy flow at $t-1$.

Charging and discharging a battery simultaneously can cause unnecessary deterioration. We also want to avoid selling and buying from the grid in the same time period. Introducing the binary variables

$$\begin{aligned} \mu_{t,m} &\in \{0,1\} && \forall t \in \mathcal{T}_m, \forall m \in \mathcal{M} \\ \pi_{t,m} &\in \{0,1\} && \forall t \in \mathcal{T}_m, \forall m \in \mathcal{M}, \end{aligned}$$

and the inequalities

$$x^{GB}_{t,m} + x^{EB}_{t,m} \leq B \cdot \mu_{t,m} \qquad \forall t \in \mathcal{T}_m, \forall m \in \mathcal{M}, \tag{20}$$

$$x^{BD}_{t,m} + x^{BG}_{t,m} \leq B \cdot (1 - \mu_{t,m}) \qquad \forall t \in \mathcal{T}_m, \forall m \in \mathcal{M}, \tag{21}$$

$$x^{BG}_{t,m} + x^{EG}_{t,m} \leq M \cdot \pi_{t,m}, \qquad \forall t \in \mathcal{T}_m, \forall m \in \mathcal{M}, \tag{22}$$

$$x^{GD}_{t,m} + x^{GB}_{t,m} \leq M \cdot (1 - \pi_{t,m}) \qquad \forall t \in \mathcal{T}_m, \forall m \in \mathcal{M}, \tag{23}$$

where M is large, we ensure these undesired events will not occur.

While introducing binary variables and their associated inequalities may appear to complicate our model, the binary constraints are only limiting the solution space to a set of sensible solutions and are not changing the convex structure.

Ensuring that the energy demand $D_{t,m}$ is consistently met is crucial, with the equation

$$x_{t,m}^{ED} + x_{t,m}^{BD} + x_{t,m}^{GD} = D_{t,m} \qquad \forall t \in \mathcal{T}_m, \forall m \in \mathcal{M},$$

it is ensured that the sum of energy bought from the grid, produced by the PV system, or drained from the battery is equal to the demand.

There is also a need for a constraint to ensure that the solar power energy exploited in the model is less than or equal to the actual production $E_{t,m}$:

$$x_{t,m}^{ED} + x_{t,m}^{EB} + x_{t,m}^{EG} \leq E_{t,m} \qquad \forall t \in \mathcal{T}_m, \forall m \in \mathcal{M}.$$

We assume that the system's owner is a *procumer* and has to keep the amount of electricity sold under a given level of A according to Norwegian regulations [50]. This level can correspond to power that exceeds the capacity of the electrical installation F, and it is crucial to consider that as a limit as well:

$$x_{t,m}^{EG} + x_{t,m}^{BG} \leq \min(A, F) \qquad \forall t \in \mathcal{T}_m, \forall m \in \mathcal{M}.$$

This study assumes $F > A$, but it is important to note that in practice, this is not necessarily true and can have implications for the potential exploitation of solar power production and should be considered.

Lastly, we have the constraints

$$x_{t,m}^{GD}, x_{t,m}^{BD}, x_{t,m}^{BG}, x_{t,m}^{GB}, x_{t,m}^{EB}, x_{t,m}^{ED}, x_{t,m}^{EG}, r_{t,m} \geq 0 \qquad \forall t \in \mathcal{T}_m, \forall m \in \mathcal{M},$$

that makes sure that all energy flows and the battery content are non-negative.

3.2.3 Objective function

The objective function of this model aims to minimize the cost considering the peak demand charge, cost per unit of energy, and the revenue from selling energy to the grid. The function consists of three terms.

The monthly peak demand charges are represented by the demand charge W_m, and the peak demand defined as

$$l_m \geq x_{t,m}^{GD} + x_{t,m}^{GB} \qquad \forall t \in \mathcal{T}_m, \forall m \in \mathcal{M}.$$

The cost of electricity is calculated by multiplying the hourly price of electricity $Q_{t,m}$ with the amount of energy bought from the grid, specifically $x_{t,m}^{GD} + x_{t,m}^{GB}$. Similarly, the revenue from selling energy to the grid is calculated by multiplying the selling price $K_{t,m}$ with the energy sold, $x_{t,m}^{BG} + x_{t,m}^{EG}$. For more details on the electricity prices, refer to Section 3.1.2.

The three terms are summed over all periods such that the complete objective function is defined as

$$\min \sum_{m \in \mathcal{M}} \left(W_m l_m + \sum_{t \in \mathcal{T}_m} Q_{t,m}(x_{t,m}^{GD} + x_{t,m}^{GB}) - \sum_{t \in \mathcal{T}_m} K_{t,m}(x_{t,m}^{BG} + x_{t,m}^{EG}) \right).$$

This section introduced a mathematical model that aims to optimize the utilization of a battery. The complete model will be summarized in Appendix B.

3.3 Stochastic model

This study investigates optimization under uncertainty of electricity demand and solar power production. To do this, we expand the deterministic model to a multistage stochastic one. This model must incorporate several recourse variables such that it is able to make corrective decisions when the uncertainty is revealed [18].

We denote the demand at time t in month m for scenario s as $\xi_{t,m}^{D}(s)$ and solar power production as $\xi_{t,m}^{E}(s)$. Note that t corresponds to one hour and not necessarily one stage. Having one separate stage for each hour would incorporate a significant amount of uncertainty but will also lead to a huge scenario tree. For instance, if we have one stage for each hour and one branching for each stage for 24 hours, the tree contains $2^{24} = 16777216$ scenarios, and the problem is computationally intractable.

To account for uncertainty in demand, we introduce the recourse variables $\alpha_{t,m,s}$ and replace the constraint

$$x_{t,m}^{ED} + x_{t,m}^{BD} + x_{t,m}^{GD} = D_{t,m} \qquad \forall t \in \mathcal{T}_m, \forall m \in \mathcal{M}$$

with the following constraint:

$$x^{ED}_{t,m,s} + x^{GD}_{t,m,s} + x^{BD}_{t,m,s} = \xi^{D}_{t,m}(s) + \alpha_{t,m,s} \qquad \forall t \in \mathcal{T}_m, \forall m \in \mathcal{M}, \forall s \in \mathcal{S}.$$

If we plan for less demand than what actually is realized, energy will be bought from the grid to ensure feasibility. Hence, $x^{GD}_{t,m,s}$ is a recourse variable. If the opposite happens, that $x^{ED}_{t,m,s} + x^{GD}_{t,m,s} + x^{BD}_{t,m,s}$ exceeds the demand, α represents the excess amount.

Similarly, to handle uncertainty in solar power production, we replace the constraint

$$x^{EG}_{t,m} + x^{EB}_{t,m} + x^{ED}_{t,m} \leq e_{t,m} \qquad \forall t \in \mathcal{T}_m, \forall m \in \mathcal{M}$$

with

$$x^{EB}_{t,m,s} + x^{ED}_{t,m,s} + x^{EG}_{t,m,s} \leq \xi^{E}_{t,m}(s) + \beta_{t,m,s} \qquad \forall t \in \mathcal{T}_m, \forall m \in \mathcal{M}, \forall s \in \mathcal{S}.$$

In this case, $x^{EG}_{t,m,s}$ is a recourse variable, such that we can always exploit solar power production. Now, $\beta_{t,m,s}$ will represent the excess amount if $x^{ED}_{t,m,s}$ and $x^{EB}_{t,m,s}$ exceed the amount of energy produced by the PV system in scenario s.

In more detail, the amount $\beta_{t,m,s}$ is redirected to be bought from the grid instead, while $\alpha_{t,m,s}$ represents excess energy and is sold. We update the objective function to incorporate the recourse variables and the scenarios. Reflecting the goal of minimum expected costs, the objective is

$$\begin{aligned}\min \quad \sum_{s\in\mathcal{S}} p_s \Bigg(\sum_{m\in\mathcal{M}} \Bigg(& W_{m,s} l_{m,s} + \sum_{t\in\mathcal{T}_m} Q_{t,m,s}(x^{GD}_{t,m,s} + x^{GB}_{t,m,s} + \beta_{t,m,s}) \\ & - \sum_{t\in\mathcal{T}_m} K_{t,m,s}(x^{BG}_{t,m,s} + x^{EG}_{t,m,s} + \alpha_{t,m,s}) \Bigg) \Bigg).\end{aligned}$$

Where p_s denotes the probability of scenario s occurring. We must also ensure that the energy sold is still under the allowed limit and that the peak demand is adjusted. By including the recourse variables in the constraints

$$x^{EG}_{t,m,s} + x^{BG}_{t,m,s} + \alpha_{t,m,s} \leq \min(A, F) \quad \forall t \in \mathcal{T}_m, \forall m \in \mathcal{M}, \forall s \in \mathcal{S} \tag{24}$$

$$l_m \geq x^{GD}_{t,m,s} + x^{GB}_{t,m,s} + \beta_{t,m,s} \quad \forall t \in \mathcal{T}_m, \forall m \in \mathcal{M}, \forall s \in \mathcal{S}, \tag{25}$$

we take into account the energy sold and peak demand adjustments. Equation (24) ensures that the energy sold does not exceed the allowed limit, while (25) adjusts the peak demand based on the energy bought from the grid and the recourse variables.

Recall the scenario tree notations from Section 2.1.3, where we defined Ω_t as the set of ω and each $s \in \omega$ is t-equivalent. The nonanticipativity constraints are added as follows

$$
\begin{aligned}
x^{GB}_{t,m,s_1} &= x^{GB}_{t,m,s_2} && \forall s_1, s_2 \in \omega, \forall \omega \in \Omega_t, \forall t \in \mathcal{T}, \forall m \in \mathcal{M} \\
x^{BG}_{t,m,s_1} &= x^{BG}_{t,m,s_2} && \forall s_1, s_2 \in \omega, \forall \omega \in \Omega_t, \forall t \in \mathcal{T}, \forall m \in \mathcal{M} \\
x^{BD}_{t,m,s_1} &= x^{BD}_{t,m,s_2} && \forall s_1, s_2 \in \omega, \forall \omega \in \Omega_t, \forall t \in \mathcal{T}, \forall m \in \mathcal{M} \\
x^{EB}_{t,m,s_1} &= x^{EB}_{t,m,s_2} && \forall s_1, s_2 \in \omega, \forall \omega \in \Omega_t, \forall t \in \mathcal{T}, \forall m \in \mathcal{M} \\
x^{ED}_{t,m,s_1} &= x^{ED}_{t,m,s_2} && \forall s_1, s_2 \in \omega, \forall \omega \in \Omega_t, \forall t \in \mathcal{T}, \forall m \in \mathcal{M},
\end{aligned}
$$

to prevent the model from exploiting future information unavailable in the current stage. Note that the decision variables $x^{GD}_{t,m,s}$ and $x^{EG}_{t,m,s}$ are not part of the nonanticipativity constraints. They depend on the revealed uncertainty and are recourse variables.

The rest of the model needs to be slightly adjusted to account for the uncertainty introduced by the stochastic variables. The complete stochastic model will be presented in Appendix C.

3.4 Scenario generation procedure

This section describes the scenario generation method. We are utilizing the machine learning algorithm Quantile Regression Forest (QRF) [51] for forecasting electricity demand and solar power production and K-means clustering [52] for constructing the scenario tree. We refer to the values used to make a prediction as *input features* and the values we aim to predict as *target values*. The data for the input features are obtained as described in Section 3.1.4 and the data for the target values in Sections 3.1.1 and 3.1.3. Data spanning from January 2021 until the beginning of February 2023 is utilized for training the forecast model.

QRF is a popular algorithm for forecasting electricity demand and renewable power generation [53]. The algorithm offers the advantage of predicting individual quantiles and is helpful when we are interested in the probability distribution and not just the average of the predicted value. The training datasets, $\boldsymbol{X}$ and $\boldsymbol{Y}$, contain the input features and corresponding target values, respectively. We train the machine learning models on these datasets such that we can map the input features to the target value and predict them accurately.

For electricity demand, the features are temperature, weekdays, and hours. While for solar power production, the features are temperature and cloud cover. Each row in the dataset corresponds to historical observations for one hour.

Given the input features, the models learn to predict the target values. The QRF is able to forecast the whole distribution of the target value, which is crucial when generating scenario trees.

We use the models to make predictions of all quantiles from 1-100 for each target value. We store these predictions in matrices, $\boldsymbol{F}$, where each row corresponds to one quantile ranging from lowest to the highest. Each column in $\boldsymbol{F}$ denotes one hour t.

This way, we have discretized the probability distribution for each target value corresponding to one-hour electricity demand and solar power production. Now we utilize K-means clustering to construct the scenario tree as similar to [54].

The tree construction process works as follows:

- Beginning at the first column of $\boldsymbol{F}$, we apply k-means clustering and group similar values into a predefined number of clusters.
- The *centroid* of each cluster represents one scenario value.
- The number of rows assigned to each cluster indicates its probability of occurring.
- We continue the clustering with the subsequent columns while increasing the number of clusters if t corresponds to a stage.
- The clustering is finished when the desired tree depth is reached.

Now, we have scenario values for each stage. These stages are connected in a sorted fashion, such that high values tend to be followed by high values. This reflects that if the value is lower than expected we assume that it will remain at a low value. However, we introduce some randomness to make the model more realistic, such that by 10 % probability, there is a random connection between the stages.

When constructing the scenario tree we assume a perfect negative correlation between solar power production and electricity demand. This assumption is made to represent the uncertainties in fewer scenarios and keep the scenario tree manageable. While it is recognized that a perfect correlation does not hold in practice, it comes from the idea that higher temperature typically yields higher solar power production and reduced need for heating in buildings.

The scenario generation procedure offers advantages, including that the QRF can discretize the distribution of the target values without making assumptions about the underlying probability distribution. However, it has weaknesses related to sensitivity to parameter choices, computational complexity, reliance on the K-Means clustering algorithm, and assuming that solar power production and electricity consumption is negatively correlated.

3.5 Comparison of stochastic, deterministic, and perfect information approaches

Stochastic programs get large with the number of scenarios and can be challenging to solve. This extra computational burden often leads to questioning whether it is worth implementing a stochastic model instead of a simpler deterministic one.

To answer these questions, we introduce two concepts, *EVPI* and *VSS*, as discussed in [18]. For calculating these values, we address the stochastic model introduced in Section 3.3 and the PHA outlined in Appendix A.

The first phase of the PHA relaxes the nonanticipativity constraints, and the scenarios are solved independently. By taking the expected value of the optimal objective function value of these solutions, we obtain the *wait-and-see* solution, denoted X_{PI}. This value quantifies the expected cost when we have perfect information about the future.

When the PHA converges, and the nonanticipativity constraints are enforced, we obtain the expected objective function value for the stochastic problem. Denoted $X_{stochastic}$.

Lastly, we obtain the *expected-value-solution*. This is done by instead of considering all scenarios in a tree, we neglect uncertainty and assume that the expected scenario will occur. These scenarios are illustrated with blue arrows in Figure 10. We denote the expected-value-solution as $X_{deterministic}$.

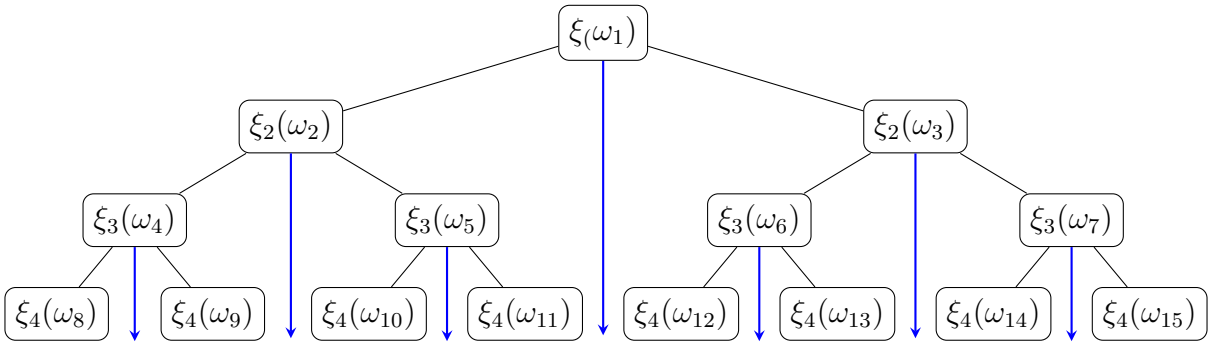

Figure 10: Multistage scenario tree and blue arrows indicating the expected scenario

Madansky [55] declared that

$$X_{\text{deterministic}} \geq X_{\text{stochastic}} \geq X_{\text{PI}}.$$

This inequality demonstrates that the expected objective function value of a stochastic solution will, at worse, be equal to the deterministic.

For comparing the performance of the two models, we calculate the VSS as

$$VSS = X_{\text{deterministic}} - X_{\text{stochastic}}.$$

The VSS indicates how much better results we can obtain by implementing a stochastic model.

In some cases we also are interested in how much better solutions we can achieve by obtaining better information about the future. This is calculated as

$$EVPI = X_{\text{stochastic}} - X_{\text{PI}}.$$

Both the EVPI and VSS can indicate if a problem requires a stochastic model [18].

By comparing the stochastic, deterministic, and perfect information approaches we aim to understand better the benefits of implementing a stochastic optimization model.

3.6 The base case

In this section, we define the base case scenario, which represents the situation without the battery, considering only the electricity demand and solar power production. We use a tilde symbol to denote variables belonging to the base case.

Let $D_{t,m}$ denote the electricity demand and $E_{t,m}$ represent the solar power production at hour t in month m. The net load, $\tilde{N}_{t,m}$, is defined as the difference between these at each hour:

$$\tilde{N}_{t,m} = D_{t,m} - E_{t,m} \qquad \forall t \in \mathcal{T}_m, \forall m \in \mathcal{M}, \tag{26}$$

where a positive net load represents energy bought from the grid, and a negative net load indicates energy sold.

We define the maximum net load for each month m, denoted as $\tilde{l}_m$, by finding the maximum value of $\tilde{N}_{t,m}$ across all hours t in that month:

$$\tilde{l}_m \geq \tilde{N}_{t,m} \qquad \forall t \in \mathcal{T}_m, \forall m \in \mathcal{M}. \tag{27}$$

By defining the base case, we establish a benchmark to better evaluate the potential cost reduction by installing and optimally operating a battery.

4 Experiments

This chapter presents the experiments. In the first case study, the deterministic model is solved with perfect information about all data. The goal is to illustrate how a battery can reduce electricity costs. However, we hypothesize that the assumption of perfect information on electricity demand and solar power production can give unrealistic expectations of such an investment.

In case studies 2 and 3, we examine two types of industrial facilities where we consider the uncertainty of electricity demand and solar power production. By comparing the stochastic approach with a simpler deterministic one, we aim if determine if a stochastic model can lower costs and, if so, to which extent.

In the last experiment, we look into the PHA. We illustrate how the value of the penalty parameter affects convergence and the objective function value and how we initialize this parameter to achieve optimal solutions.

All experiments are executed on a computer with 11th Gen Intel(R) Core(TM) i7-1165G7 2.80GHz processor, 16GB RAM, and 64-bit Windows 10 Pro operating system using Gurobi 9.5.2 [56].

4.1 Case study 1: Deterministic analysis with perfect information

This section utilizes the deterministic model outlined in Section 3.2. By combining a PV system with battery storage and having perfect information about electricity demand, solar power production, and spot prices, this case study aims to investigate how a battery reduces costs by peak shaving and price arbitrage operations and to what degree.

We focus on an office building located on the west coast of Norway and the base case described in Section 3.6. The data from the whole of 2022 is utilized such that the set $\mathcal{M} = \{1, 2 \ldots, 12\}$ and $\mathcal{T}_m$ represent all hours of the month m. Data for electricity demand, prices, and solar power production is described in Sections 3.1.1-3.1.3 and the parameters used are presented in Table 2.

Table 2: Case Study 1 parameters

PVGIS Inputs		**Other Parameters**	
PV system capacity	100 kWp	Battery capacity[B]	100 kWh
Longitude	60.36°	Maximum net grid injection [A]	100 kWh
Latitude	5.35°	Spot price area	NO5
Surface-tilt	10°		
Surface-azimuth	90°		
Loss	14%		

Table 3 shows the experienced costs in 2022 for the base case along with the optimal objective function value for each month, demonstrating the potential cost reduction that can be achieved by installing a battery.

Table 3: Case study 1 results

Month	**Total cost without battery [NOK]**	**Total cost with battery [NOK]**	**Reduction [NOK]**	**Reduction [%]**
1	65838	63902	1935	2.94
2	56834	55090	1744	3.07
3	68069	64645	3423	5.03
4	50497	48279	2218	4.39
5	51054	48179	2874	5.63
6	49570	46587	2982	6.01
7	45739	42843	2896	6.33
8	99772	95238	4533	4.54
9	94656	85701	8954	9.46
10	49475	45693	3781	7.65
11	42217	38943	3273	7.75
12	112225	106812	5413	4.82
Total	785940	741912	44026	5.60

Table 3 illustrates that the cost reduction achieved with the model equals 44,026 NOK, with the monthly savings ranging from 1,744 NOK in February to 8,954 NOK in September. The

variation in monthly cost reduction is quite high, and we are investigating why this is the case.

Figure 11 illustrates the net load for both the base and optimal cases. Recall from Equation (26) in Section 3.6 the definition of the net load $\tilde{N}_{t,m}$ for the base case, as the difference between the electricity demand and solar power production. And for the optimal case, the net load is given by $x^{GB}_{t,m} + x^{GD}_{t,m} - x^{EG}_{t,m} - x^{BG}_{t,m}$.

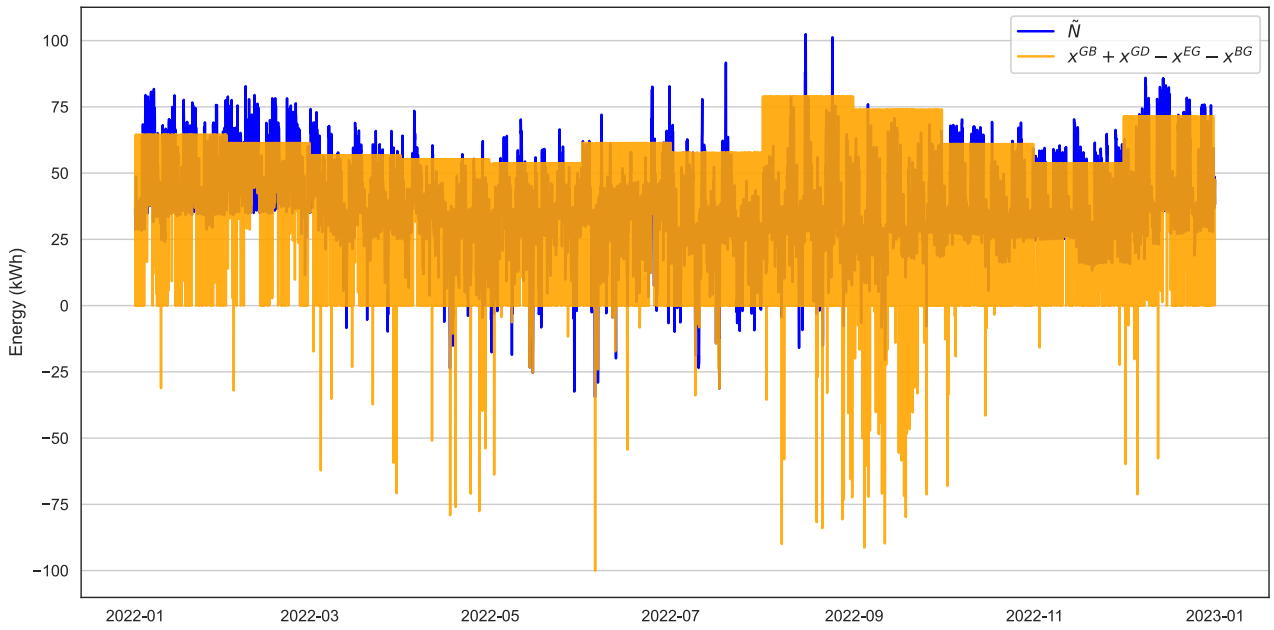

Figure 11: Comparison of net load during 2022 with and without battery storage

The figure displays net load demand for the base case and net load for the optimal case, one value for each hour in 2022 with unit kWh. The base case shows a relatively high net load during daytime hours and a relatively low net load during nighttime and weekends. During the summer months, negative values are observed because the production from the PV system exceeds the electricity demand. On the other hand, in the optimal case, we see a spikey pattern, with each month displaying a consistent peak demand that holds through the month. We also observe that negative values in the optimal case are not constrained to hours of solar power production.

4.1.1 Peak Shaving

Figure 12 shows how the battery affects the peak demand for each month. The figure compares the peak demand for the base case $\tilde{l}_{t,m}$ and the optimal case $l_{t,m}$.

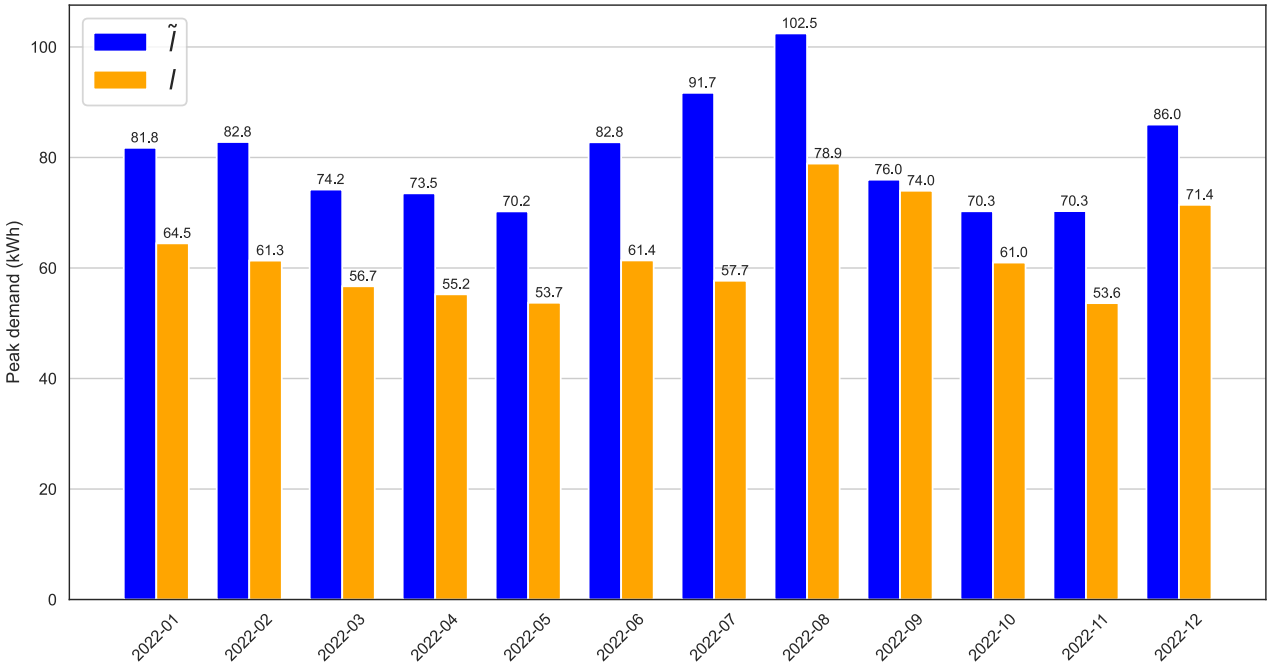

Figure 12: Monthly peak electricity demand during 2022

We see that when optimally operating a battery with perfect information, the peak demand is reduced every month. The most significant reduction is in July, and in September, the peak is only slightly reduced.

Figures 13a and 13b illustrate the same as Figure 11, zoomed in on February 10 and July 10, respectively.

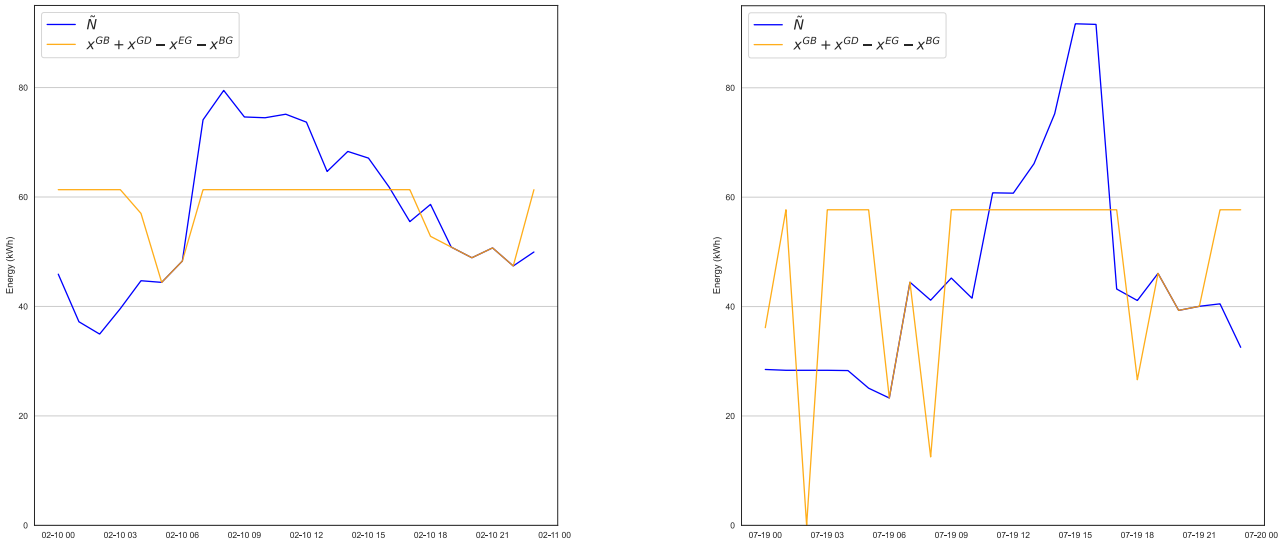

(a) Dense peak

(b) Light peak

Figure 13: Comparison of light and dense peak

In Figure 13a, there is a dense peak, meaning that the volume of the electricity demand is spread out over multiple hours, while on July 10, the peak is lighter such that the peak demand charge can be reduced more with an equal amount of battery capacity. This demonstrates that the shape of the electricity demand is vital for how much it is possible to reduce the peak demand charge with a battery and aligns with the findings in [36, 37].

To comprehend the relatively low peak shaving observed in September, examining the price arbitrage operations that may coincide with peak shaving is necessary.

4.1.2 Price arbitrage

In Figures 14a and 14b, the average price of electricity bought and sold, measured in NOK per kWh, is visualized along with the average spot price in the same period.

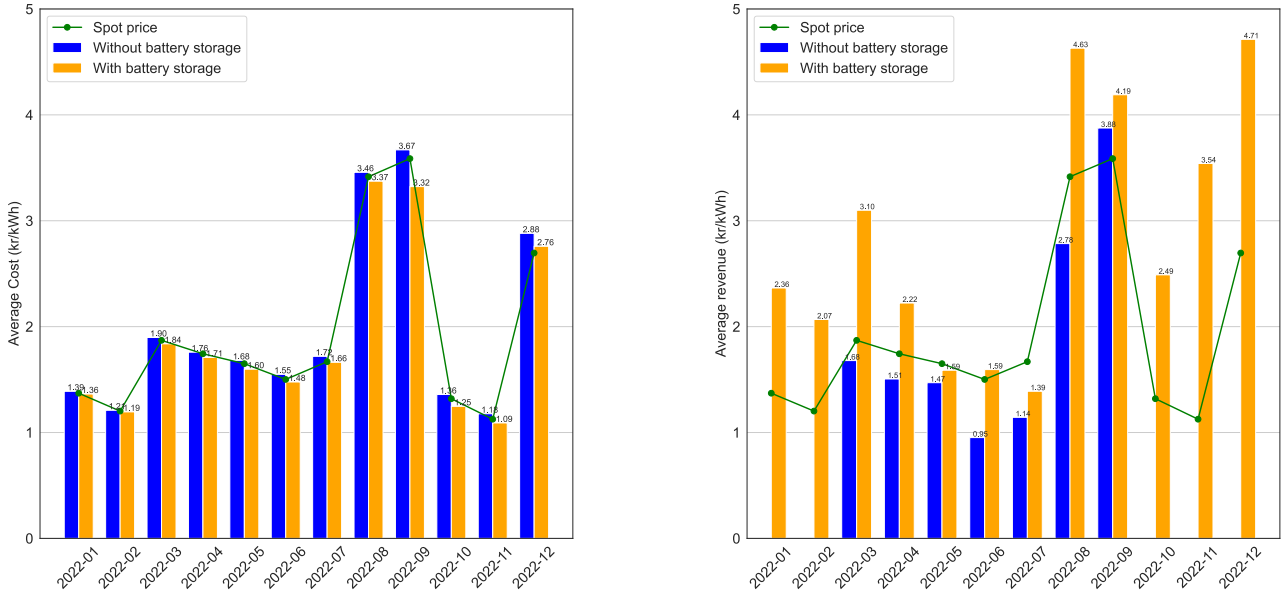

(a) Average spot price of electricity purchased from the grid during 2022

(b) Average revenue from selling electricity to the grid during 2022

Figure 14: Comparison of average spot prices and revenues for electricity transactions in 2022

The figures show that the model can reduce the average purchase price and raise the average electricity sales revenue. At the same time, it is shown that the average purchase price is less affected compared to the average revenue. This is because the battery's capacity is relatively low compared to the amount of energy bought from the market. The difference in average revenue is more significant than the average buying price. This is because when solar power production exceeds the demand in the base case, the production is sold regardless of the spot price in that period. An optimally operated battery can charge and wait until the price reaches

a sufficiently high level before the energy content is sold to the grid.

To better understand why the reduced costs are that high in September, we investigate the spot price volatility, as introduced in Section 3.1.2.

Figure 15 visualizes the volatility of the spot price. Each bar represents the average daily standard deviation for each week.

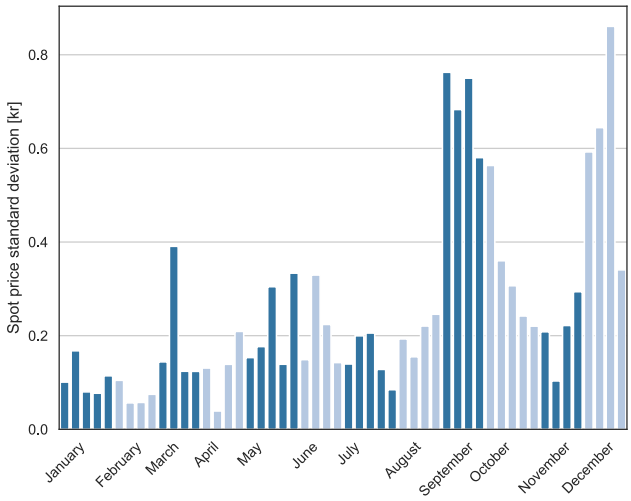

Figure 15: Spot price volatility in 2022

The volatility is relatively high in September and December and relatively low from January to August, which can explain the reduced costs in September. Looking back at Figure 11, we see that the net load for the base case is relatively low in that month, such that the battery can use more of the capacity of doing price arbitrage operations and take advantage of the high volatility. We expect to see the same amount of price arbitrage operations in December. However, Figure 11 reveals that the net load is much higher this month, and the optimal exploitation of the battery prioritizes peak shaving.

To better illustrate how the battery reduces costs, the reduction percentage from Table 3 is split up in Table 4. We can identify some trade-offs between peak shaving and price arbitrage operations during high volatility, especially in September and December. And we can also see that price arbitrage is the largest contributor to cost reduction. This finding deviates from [41], where peak shaving led to 95.6 % of the reduced electricity bill. There can be multiple reasons for this, including the different demand patterns and the fact that the spot price volatility in 2022 was especially high.

Table 4: Monthly total electricity cost reduction percentages resulting from peak shaving and price arbitrage operations

Month	Peak shaving [%]	Price arbitrage [%]	Month	Peak shaving [%]	Price arbitrage [%]
1	1.55	1.39	7	3.64	2.69
2	2.23	0.84	8	1.16	3.39
3	1.52	3.51	9	0.10	9.36
4	1.77	2.62	10	1.11	6.54
5	1.59	4.04	11	2.33	5.43
6	2.11	3.90	12	0.76	4.06

4.1.3 One week

To get a better understanding of how the battery is contributing to reducing costs and to be able to study the operation in more detail, we examine one week from August 12th to August 19th. Figure 16a presents the same as Figure 11, focusing on this specific week. This figure shows a relatively low net load $\tilde{N}_{t,m}$ during the first three days, where negative values indicate that solar power production exceeds demand. Moreover, we see a substantial peak in net load on August 15th, indicating large electricity demand and relatively low solar power production.

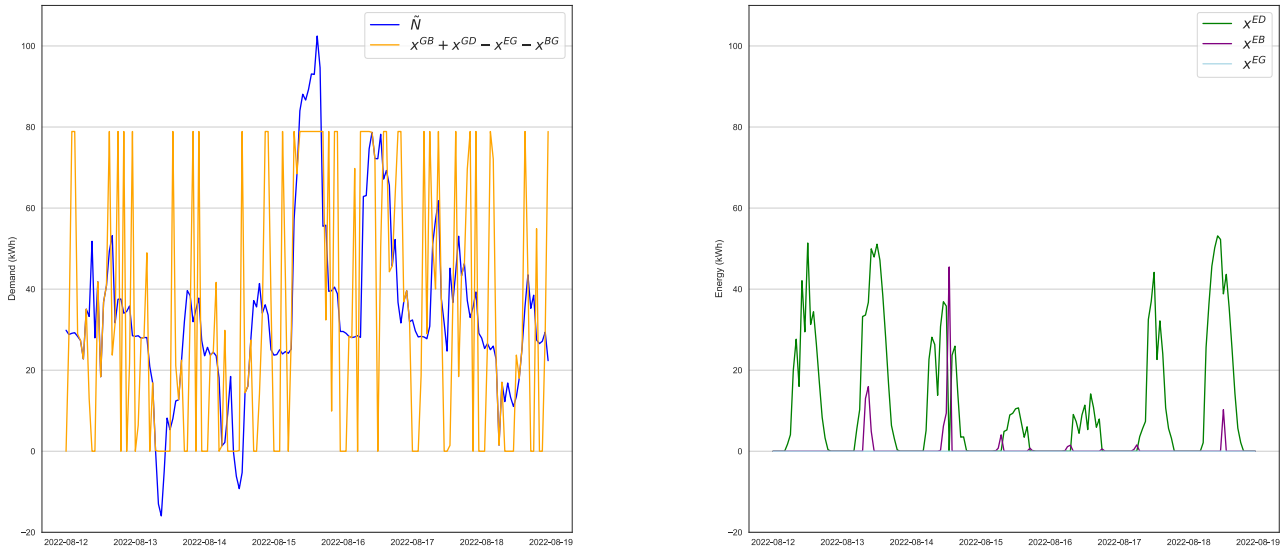

(a) Net load for the base case and the optimal case

(b) Solar power production

Figure 16: Net load and solar power production

When we look at the net load for the optimal case, the pattern is quite different from the base case. The optimal net load is very spikey, which shows the relatively cheap hours when the battery charges up. When there are no spikes in the net load, the battery is discharging. One interesting point is how the peak in $\tilde{N}_{t,m}$ during the middle of the week gets shaved off in the optimal case. This is the only time in this period when the battery is used for peak shaving. The battery is utilized for price arbitrage operations rather than peak shaving for the rest of the time.

The values of the decision variables corresponding to solar power production are visualized in Figure 16b. The figure shows that the production of the PV system was relatively high on five days of that week. The figure also shows that most of the production is assigned to $x_{t,m}^{ED}$, and nothing is sold to the grid during this period. When comparing this with Figure 16a, we see that energy is only used for charging the battery when the net load in the base case is negative. This illustrates that the optimal exploitation of solar power production is to cover the demand and that the spot price is not sufficiently high during this period.

Figures 17a and 17b illustrate the values of the variables corresponding to the battery and the spot price during the same period. Figure 17a shows the battery charging from the grid, while Figure 17b displays the battery discharging.

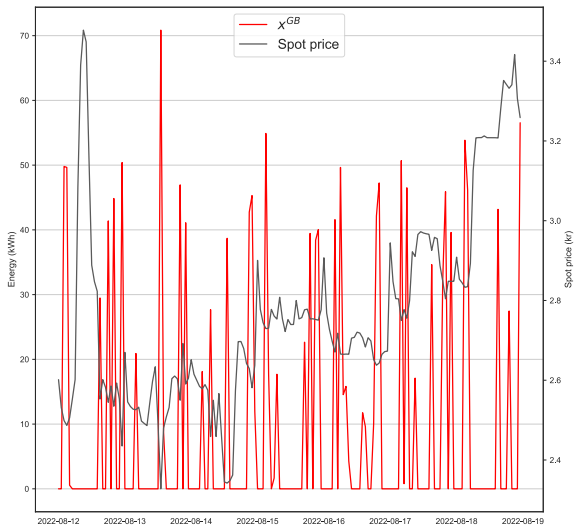

(a) Energy flow from the grid to the battery

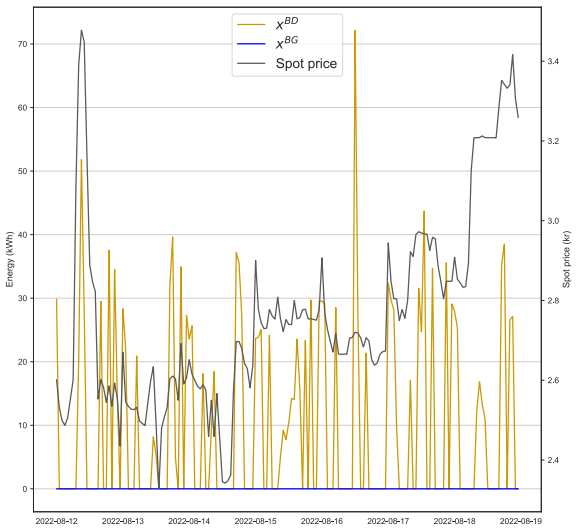

(b) Energy flow from the battery to the demand and the grid

Figure 17: Battery decision variable values

The plots show the battery charges in periods with a relatively the spot price and discharges when the price increases. Notably, no energy is sold from the battery to the grid, emphasizing

that covering the demand is prioritized.

This study investigates how an optimally operated battery and a PV system reduce electricity costs. Despite possessing perfect information on all parameters, we can draw some interesting findings from this case study.

Optimally exploiting a 100 kWh battery reduces costs by 44025 NOK, or 5.60%, on 2022 data. This is done by utilizing both peak shaving and price arbitrage operations.

The analysis shows that the shape of the electricity demand is crucial for the amount of peak shaving being done within a billing period. Lighter peaks lead to more demand charge reduction compared to months with denser peaks. Additionally, the economic potential of utilizing a battery for price arbitrage operations is sensitive to spot price volatility which can vary substantially during a year.

However, this case study might have limited generalizability because of the assumption of perfect information. In the following two case studies, we investigate how uncertainty can influence the economic potential of battery installations.

4.2 Stochastic approach

In the following case studies, we investigate the results from the stochastic model as presented in Section 3.3.

As before, the consumption data, solar power production data, and electricity prices are obtained as described in Section 3.1.

We use scenario trees to represent demand and solar power production. We recall from Section 2.1.3 the scenario tree notation, represented by the equivalence classes ω, the set of equivalence classes Ω_t, and the set of scenarios $\mathcal{S}$, which we utilize to model uncertainties. We also refer back to Section 3.3 to recall the scenario notations for demand and solar power production, denoted by $\xi^D_{t,m}(s)$ and $\xi^E_{t,m}(s)$ respectively.

Also, be reminded of the Algorithm 1 and the concept of δ and k_{max} as explained in Section 2.1.4. The results of the stochastic optimization model lead to the determination of $X_{deterministic}, X_{stochastic}, X_{PI}, EVPI$, and VSS as introduced in Section 3.5.

4.2.1 Case Study 2: An office building

In this extension of Case Study 1 from Section 4.1, we now investigate the same industrial facility under a stochastic setting, where the electricity demand $D_{t,m}$ and solar power production $E_{t,m}$ are uncertain.

For this case study, we focus on February 1, 2023, to evaluate the performance of the stochastic optimization model. The parameters of this case study are shown in Table 5.

Table 5: Case Study 2 parameters

PVGIS Inputs		**Other Parameters**	
PV system capacity	100 kWp	Battery capacity [B]	50 kWh
Longitude	60.36°	Maximum net grid injection [A]	100 kWh
Latitude	5.35°	$\mathcal{M}$	{Feb}
Surface-tilt	10°	$\mathcal{T}_m$	1 - 24
Surface-azimuth	90°	Year	2023
Loss	14%	Spot price area	NO5
		Max iterations [k_{max}]	200
		Convergence criterion [δ]	0.1
		Penalty parameter [ρ]	1

Our scenario trees that represent $\xi^D_{t,m}(s)$ and $\xi^E_{t,m}(s)$ are generated and combined using the method described in Section 3.4 and are illustrated in Figure 18.

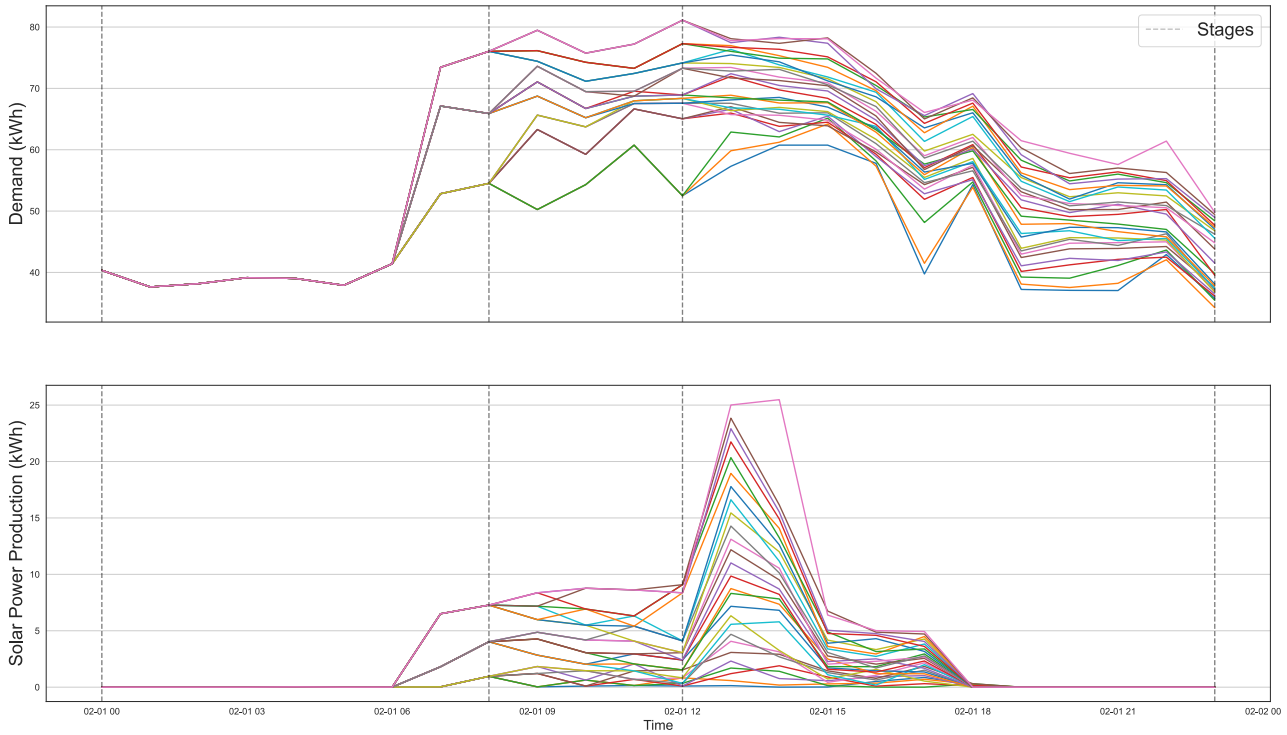

Figure 18: Scenario trees for electricity demand and solar power production

The scenario tree is constructed by 27 scenarios such that,

$$|S| = 27$$

$$\omega_1 = \{s_1, s_2, ..., s_{27}\}$$

$$\omega_2 = \{s_1, ..., s_9\}, \omega_3 = \{s_{10}, s_{11}, ..., s_{18}\}, \omega_4 = \{s_{19}, ..., s_{27}\}$$

$$\omega_5 = \{s_1, s_2, s_3\}, \omega_6 = \{s_4, s_5, s_6\}, \omega_7 = \{s_7, s_8, s_9\}, \omega_8 = \{s_{10}, s_{11}, s_{12}\}\omega_9 = \{s_{13}, s_{14}, s_{15}\},$$

$$\omega_{10} = \{s_{16}, s_{17}, s_{18}\}, \omega_{11} = \{s_{19}, s_{20}, s_{21}\}, \omega_{12} = \{s_{22}, s_{23}, s_{24}\}, \omega_{13} = \{s_{25}, s_{26}, s_{27}\}$$

$$\Omega_8 = \{\omega_1\}, \Omega_{12} = \{\omega_2, \omega_3, \omega_4\},$$

$$\Omega_{23} = \{\omega_5, \omega_6, \omega_7\, \omega_8, \omega_9, \omega_{10}, \omega_{11}, \omega_{12}, \omega_{13}\}$$

The first decision is made at $t = 0$. It is both low electricity demand and solar power production during the night, so the second stage is set at $t = 8$, the third stage at $t = 12$, and the final stage at $t = 23$.

Including a larger tree with more stages and finer branching can improve the representation of the uncertainty and a more realistic decision-making process, but as the number of scenarios increases, the model size grows and increases the computational burden.

We set the convergence criterion at $\delta = 0.01$ and the maximum number of iterations to $k_{max} = 200$. The results of the case study are presented in Table 6.

Table 6: Case Study 2 results

Metric	Value	Metric	Value
$X_{deterministic}$	5258 NOK	$EVPI$	55 NOK
X_{PI}	4957 NOK	VSS	246 NOK
$X_{stochastic}$	5012 NOK	Running time	7900 s

In Table 6, it is shown that the values of both VSS and EVPI are quite low. There can be multiple reasons for low values of VSS and EVPI. The scenario tree we are using to represent electricity demand and solar power production might not be able to fully incorporate the uncertainties, which can lead to relatively similar solutions across the scenarios.

Additionally, more than one 24-hour window might be required to evaluate the benefits of considering uncertainty in this case. This can also indicate that the scenario generation method is not effectively capturing the randomness. But it could also suggest that the problem is less sensitive to uncertainties, meaning that the benefits of a stochastic approach over a simpler deterministic one are limited.

The next section investigates how the stochastic approach performs in an industrial facility with more uncertainty.

4.2.2 Case Study 3: An energy-intensive industry

This case study investigates applying the stochastic model and the PHA to a consumption pattern inspired by an energy-intensive industry, specifically a crushing mill. The purpose is to explore the differences between the stochastic and deterministic approaches and how stochasticity in electricity demand affects the solution.

As the assumption of a negative correlation between electricity demand and solar power production is not valid in this context, we set

$$\xi^{E}_{t,m}(s) = 0 \qquad \forall t \in \mathcal{T}_m, \forall m \in \mathcal{M}, \forall s \in \mathcal{S}.$$

This case study examines a site with high electricity demand and without a PV system. Therefore, we do not consider parameters from PVGIS. Since the demand is relatively high, we set the battery capacity to 1000 kWh. The parameters used in this study are described in Table 7.

Table 7: Case Study 3 parameters

Parameters	
Battery capacity [B]	1000 kWh
Maximum net grid injection [A]	100 kWh
$\mathcal{M}$	{Feb}
$\mathcal{T}_m$	1-24
Year	2023
Spot price area	NO5
Max iterations [k_{max}]	1000
Convergence criterion [δ]	0.1
Penalty parameter [ρ]	1

The problem is simplified by focusing on eight scenarios for $\xi^D_{t,m}(s)$, structured into four stages as follows:

$$
\begin{aligned}
S &= \{s_1, s_2, s_3, s_4, s_5, s_6, s_7, s_8\} \\
\omega_1 &= \{s_1, s_2, s_3, s_4, s_5, s_6, s_7, s_8\} \\
\omega_2 &= \{s_1, s_2, s_3, s_4\}, \omega_3 = \{s_5, s_6, s_7, s_8\} \\
\omega_4 &= \{s_1, s_2\}, \omega_5 = \{s_3, s_4\}, \omega_6 = \{s_5, s_6\}, \omega_7 = \{s_7, s_8\} \\
\Omega_{12} &= \{\omega_1\}, \Omega_{16} = \{\omega_2, \omega_3\}, \Omega_{18} = \{\omega_4, \omega_5, \omega_6, \omega_7\} \\
\Omega_{23} &= \{\omega_i : i \in \{8, 9, ..., 15\}\}, \quad \text{where } \omega_i = \{s_{i-7}\} \quad i = 8, ..., 15
\end{aligned}
$$

The actual values of the uncertain demand are drawn randomly from a uniform probability

distribution specified as follows:

$$\xi^D_{t,m}(s) \sim U(10,12) \quad \forall s \in \omega_1, 0 \leq t \leq 5$$
$$\xi^D_{t,m}(s) \sim U(10,12) \quad \forall s \in \omega_2, 6 \leq t \leq 11$$
$$\xi^D_{t,m}(s) \sim U(210,220) \quad \forall s \in \omega_3, 6 \leq t \leq 11$$
$$\xi^D_{t,m}(s) \sim U(10,12) \quad \forall s \in (\omega_4 \cup \omega_6), 12 \leq t \leq 15$$
$$\xi^D_{t,m}(s) \sim U(210,220) \quad \forall s \in (\omega_5 \cup \omega_7), 12 \leq t \leq 15$$
$$\xi^D_{t,m}(s) \sim U(10,12) \quad \forall s \in (\omega_8 \cup \omega_{10}, \omega_{12} \cup \omega_{14}), 16 \leq t \leq 17$$
$$\xi^D_{t,m}(s) \sim U(210,220) \quad \forall s \in (\omega_9 \cup \omega_{11}, \omega_{13} \cup \omega_{15}), 16 \leq t \leq 17$$
$$\xi^D_{t,m}(s) \sim U(10,12) \quad \forall s \in S, 18 \leq t \leq 23$$

All the scenarios are illustrated in Figure 19, where each node denotes the value for $\xi^D_{t,m}$ up to that stage. All scenarios have an equal probability of occurrence.

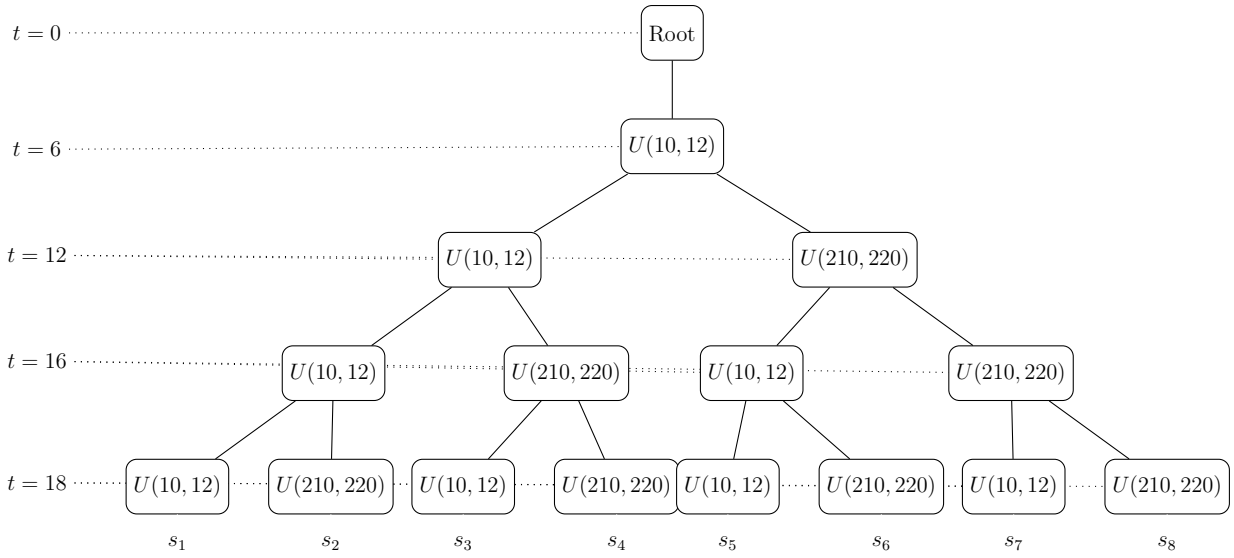

Figure 19: Case Study 3 scenario tree

The metrics, $X_{deterministic}, X_{stochastic}, X_{PI}, EVPI$, and VSS are calculated, and the results are presented in Table 8.

The data in Table 8 shows that a stochastic approach reduces the costs by 1583 NOK, or 15.3%, compared to the deterministic model that ignores uncertainty. This underscores that it is important to consider the uncertainties of electricity demand to optimally reduce costs in this case. The EVPI of 3561 NOK indicates that it is not valid to assume perfect information and that it is crucial to consider this uncertainty before investing in a battery for cost-reduction

Table 8: Case Study 3 results

Metric	Value	Metric	Value
$X_{deterministic}$	11957 NOK	$EVPI$	3561 NOK
X_{PI}	6813 NOK	VSS	1583 NOK
$X_{stochastic}$	10369 NOK	Running time	7206 s

purposes. We look closer at one of the scenarios to better understand why the VSS and EVPI are so high.

In Figures 20 to 22, we illustrate the rightmost scenario s_8 from the scenario tree presented in Figure 19, along with the solutions. The scenario s_8 represents a situation where we observe high values continuously from $t = 6$ to $t = 18$. Specifically, we examine the sum $x^{GB}_{t,m} + x^{GD}_{t,m} + \beta_{t,m}$, which represents the total amount of energy purchased from the grid, and $x^{BG}_{t,m} + \alpha_{t,m}$, which denotes the total amount of energy sold.

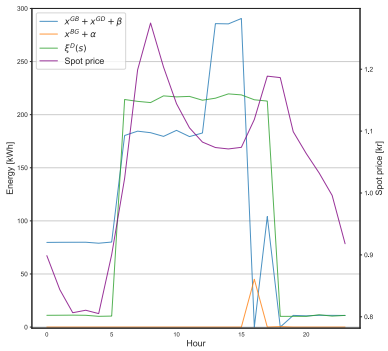

Figure 20: Deterministic results

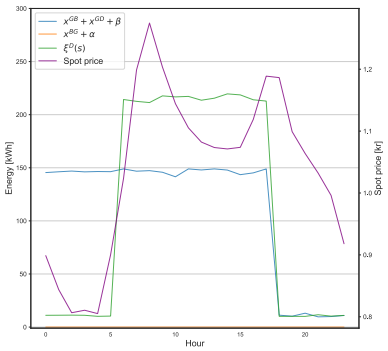

Figure 21: Stochastic results

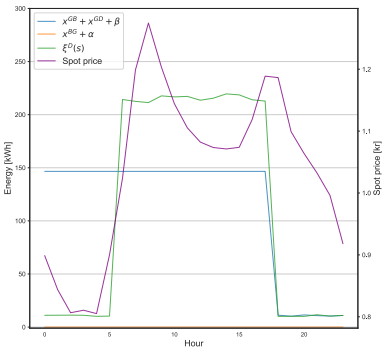

Figure 22: Perfect information results

In this scenario, the stochastic model is able to reduce costs substantially compared to a deterministic one. That is because the model can weigh the consequences of both high and low scenarios. In this case, the optimal solution is prioritizing shaving off the peak instead of price arbitrage operations. The deterministic model assumes the expected scenario and underestimates the actual electricity demand. By underestimating the demand, the battery is getting charged during hours with already high consumption, and that strategy leads to a costly peak demand charge.

For this specific scenario, we can see that the solutions for the stochastic approach and perfect information are similar. To understand better why the EVPI is high, we must investigate the

solution for the other scenarios.

Figure 23 presents the objective function values for the stochastic, deterministic, and perfect information approaches across all eight scenarios.

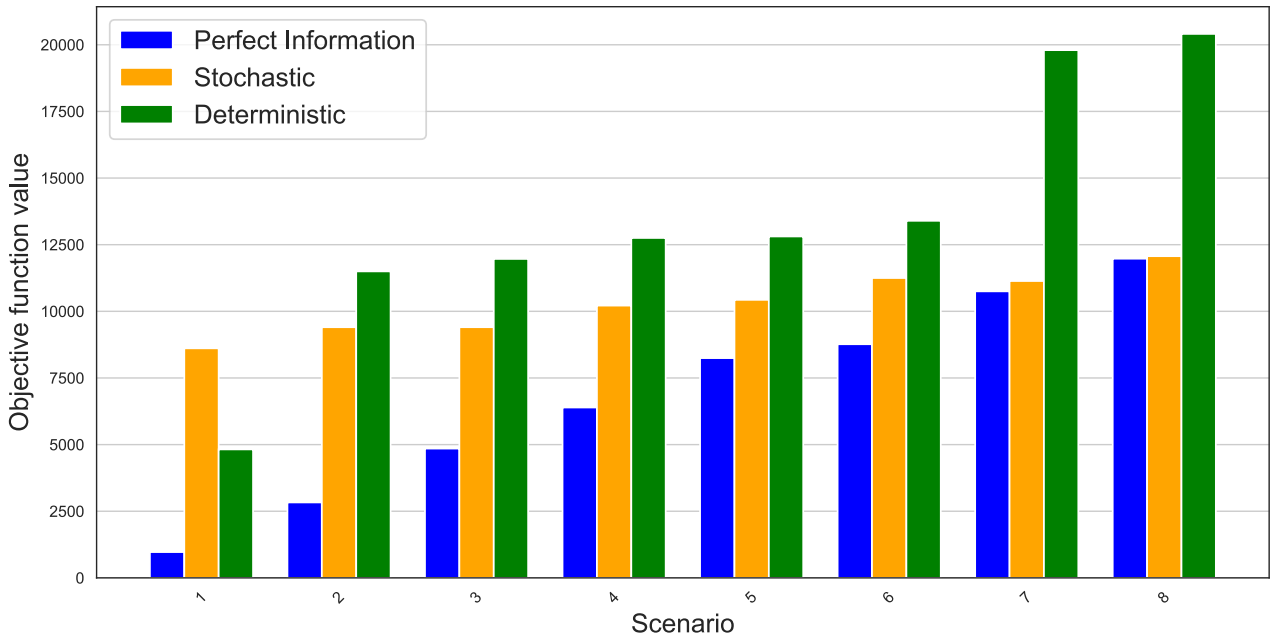

Figure 23: Objective function values

The bar chart illustrates that the stochastic approach finds better solutions in seven of the eight scenarios compared to the deterministic model.

We also see that the difference between the objective function value of the stochastic model and the approach with perfect information is similar in scenarios where $\xi^D_{t,m}(s)$ is high and not so close for scenarios with low demand. This relationship illustrates that the stochastic model weighs the consequences of all the scenarios and converges against a solution that is robust to high demand and, as a cost, performs worse in scenarios with low electricity demand. By that, we can see that the optimal decision is not to assume the expected scenario when uncertain since underestimating the future electricity demand can be relatively expensive.

In conclusion, this case study highlights the advantages of using a stochastic model for battery management for an energy-intensive industry. This case study shows that a simpler deterministic model that ignores uncertainty leads to an additional cost of 1583 NOK or 15.3%. And the costs can be reduced by as much as 3561 NOK, or 34.3%, with more information about the scenarios.

This suggests that assuming perfect information is invalid when analyzing the potential electric-

ity cost reductions in this case. Also, this value indicates how much it is possible to additionally reduce the costs by getting better information about the scenarios. This can be done by, for instance, consulting with the operator of the industrial facility or investing in forecast models.

When interpreting the results one should keep in mind that the model operates within a 24-hour window. This means that while these savings are relatively high, the daily cost reduction will be less since the billing cycle of the peak demand charge is monthly. The optimal exploitation of the battery, in this case, will be to empty its content within the time window. In practice, it could save energy beyond this time period.

4.3 Initializing the penalty parameter in the Progressive Hedging Algorithm

This experiment focuses on the PHA. In Section 2.1.4, we discuss how the value of ρ can significantly impact the algorithm's convergence and that while multiple strategies for assessing the value of this parameter exist, there is no consensus on an optimal approach. This experiment will explore how varying ρ affects our problem. Case study 3 is used as an illustrative example, and a similar approach is done for initializing ρ in case study 2.

In this study, we initialize the parameter to a fixed value $\rho > 0$. To determine the appropriate value for the parameter, we test a range of values between 0.01 and 50.

Remember that k, denotes the current iteration number, while the convergence criterion, δ, measures how close a solution is to feasibility. The value of ρ can influence the number of iterations needed to meet this convergence criterion.

Figures 24a - 24b illustrate δ the first 200 and last 200 iterations of a total number of 1000 iterations of the PHA. We have set the maximum number of iterations to 1000 to keep the running time approximately two hours for each value.

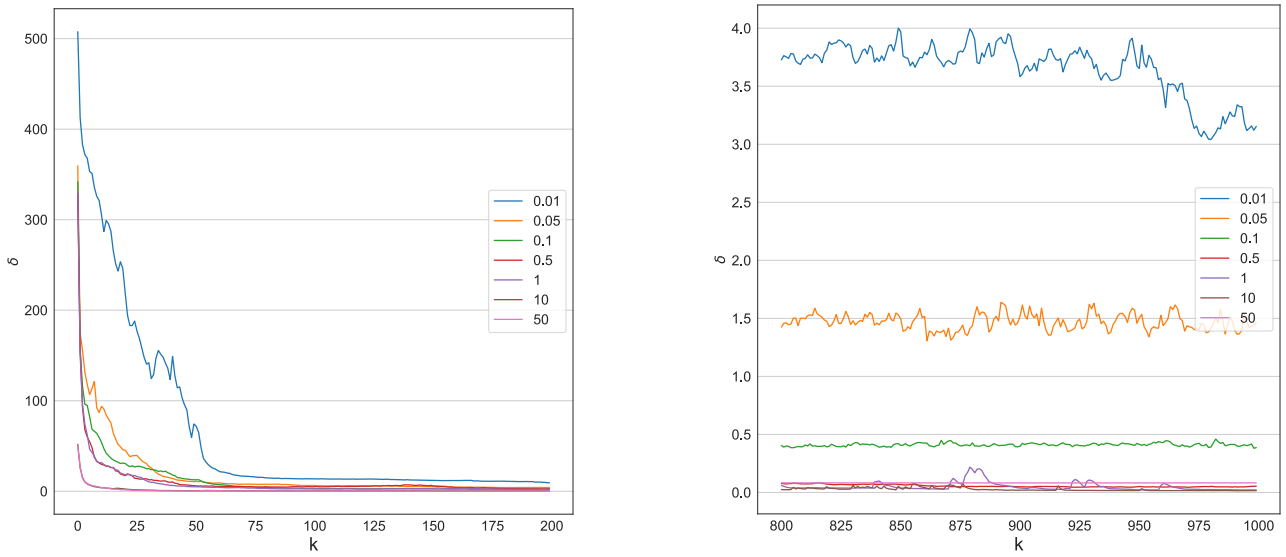

(a) Iterations 0-200

(b) Iterations 800-1000

Figure 24: Distance plots for different values of ρ during the first 200 iterations and the last 200 iterations

In Figure 24a, we notice that when initializing with a low value for ρ, the PHA starts with a less implementable solution. In other words, the nonanticipativity constraints are not enforced. When initializing with higher values, the algorithms find solutions closer to feasibility faster. These findings are expected as described in [27].

In Figure 24b, we observe that the values of $\rho < 0.5$ still have a noticeable distance from $\delta = 0$, while $\rho \geq 0.5$ is close to convergence.

In Figures 25a - 25b, the objective function value in the first and last 200 iterations of the algorithm is illustrated. In Figure 25a, we observe that the lower the penalty parameter we start with, the lower the objective function value is.

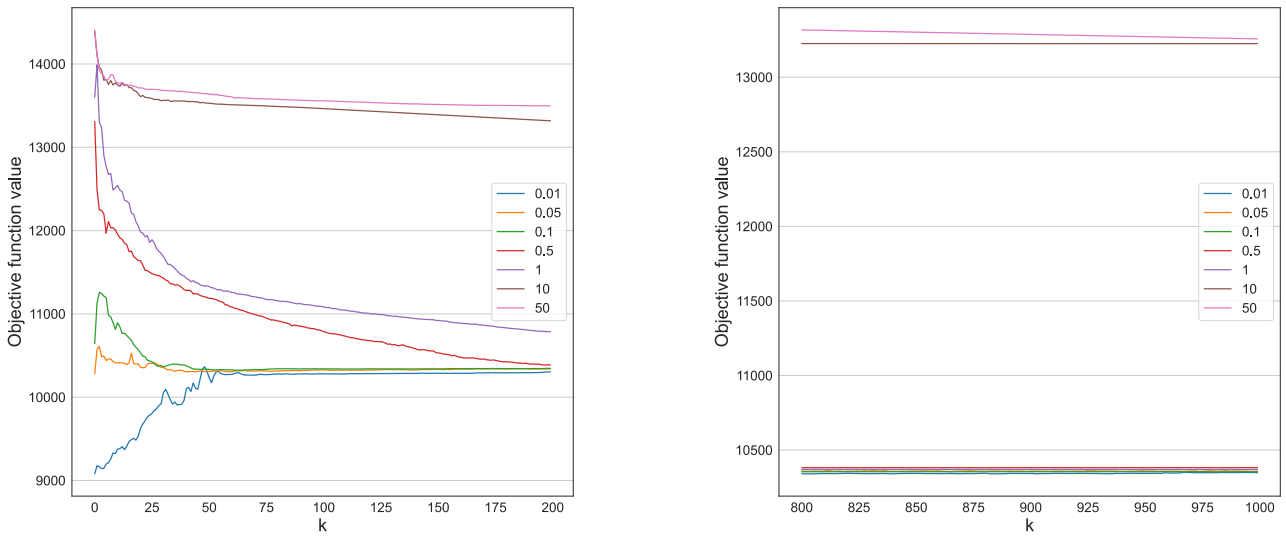

(a) Iterations 0-200

(b) Iterations 800-1000

Figure 25: Objective function value plots for different values of ρ during the first 200 iterations and the last 200 iterations

Recall from the value of $X_{PI} = 6813$ from Table 8 in Section 4.2.2. A low initializing of ρ will penalize the deviation from this solution relatively little, so we start close to that solution. However, as shown in Figure 25a, this solution is far from feasible, and the algorithm slowly converges toward an implementable solution.

On the contrary, a large initializing of ρ makes the algorithm start with a solution with a high objective function value; however, as we see in Figure 25a, it is also a solution closer to feasibility.

In Figure 25b, we notice that the objective function value for solutions with $\rho \geq 10$ is much larger than for the rest of the penalty parameters.

In conclusion, in this experiment, we have seen that implementations with penalty parameters $\rho < 0.5$ do not converge sufficiently close to $\delta = 0$ within the $k_{max} = 1000$ iterations. We also observed that solutions with $\rho \geq 10$ lead to sub-optimal convergence. We observe that we get similar solutions for $0.5 \leq \rho \leq 1$, and we initialize the parameter to 1.

5 Conclusion and future work

This study examines how optimally operated batteries can reduce the electricity bill for industrial facilities and how the uncertainty of electricity demand and solar power production affects these cost reductions. We address these questions by implementing both deterministic and stochastic optimization models.

The results of the first case study demonstrate that electricity costs are reduced both by peak shaving and price arbitrage operations. The degree of reduction depends on the electricity demand's shape and the spot price's volatility. Our deterministic analysis with perfect information demonstrates that the cost was reduced by 5.60%, compared to the base case, using 2022 data. This analysis highlights that it is crucial to consider both price arbitrage and peak shaving when minimizing costs utilizing a battery.

Extending the deterministic model into a multistage stochastic optimization model allows us to assess the impact of uncertain electricity demand and solar power production. Our results illustrate the extent to which the EVPI and the VSS vary with the degree of uncertainty. If the uncertainty is sufficiently low, a deterministic may suffice, and it is not necessary to complicate the model with stochasticity.

However, the case study in Section 4.2.2 with relatively high uncertainty in the electricity demand results in a cost reduction of 1583 NOK when comparing a stochastic approach to a simpler deterministic model that ignores uncertainty. The same case study demonstrated an EVPI of 3561 NOK which underscores that it is not always valid to assume perfect information when evaluating how much a battery installation can reduce electricity costs.

While the results give valuable insights into optimal battery operation and the implications of uncertainty, some limitations of this study should be acknowledged.

Only hourly resolution data were available for this study. More granulated data can be increasingly available because of the vast implementation of HAN-adapters. Possessing finer-resolution data can lead to a more realistic analysis of the battery operation. It can also help address additional questions, such as optimal dimensioning of the battery capacity and power.

The battery model is relatively simple, and ignoring battery degradation impacts battery exploitation. Also, degradation can affect the battery's capacity and energy efficiency over time. A potential model improvement can be to include a more comprehensive battery model.

Our study considered two 24-hour windows only. This will give end-of-horizon issues to some

degree. Future research could reduce these issues by implementing larger time windows or a rolling horizon approach. This can provide additional knowledge about the benefits and limitations of a stochastic approach. A rolling-horizon approach can also be more practical-oriented since the decision made at the first time period is likely the only one being implemented.

However, the mentioned additions come with an increasing complexity and model size, which increases the computational time. Future studies can research alternatives to the PHA, either exact or good approximations.

Future studies can also investigate developing a more case-specific scenario generation method. By consulting with human experts close to the operation of a facility, it can be possible to gain additional knowledge about the uncertainty of the electricity demand and represent the underlying distribution with relatively few scenarios.

References

[1] Statnett. *Områdeplan Nord: Nordre Nordland, Troms og Finnmark*. Statnett. September. Norway, 2022.

[2] BKK. *Regional Kraftsystemutredning for BKK-området og indre Hardanger*. Tech. rep. BKK, 2020.

[3] Magnus Buvik et al. *Norsk og nordisk effektbalanse fram mot 2030*. Tech. rep. 20/2022. NVE, 2022.

[4] The Norwegian Water Resources and Energy Directorate. *Ny nettleie (fra 1. juli 2022)*. Retrieved from `https://www.nve.no/reguleringsmyndigheten/kunde/nett/ny-nettleie-fra-1-juli-2022/`. Last updated on July 1, 2022. July 2022.

[5] *Sol-data fra Elhub*. Tech. rep. Updated on May 2, 2023. Norway: Elhub, May 2023. URL: `https://elhub.no/app/uploads/2023/05/ManedsrapportSOL.pdf`.

[6] Olukunle O Owolabi et al. "A robust statistical analysis of the role of hydropower on the system electricity price and price volatility". In: *Environmental Research Communications* 4.7 (2022), p. 075003.

[7] International Energy Agency. *Renewables 2022*. License: CC BY 4.0. Paris, 2022. URL: `https://www.iea.org/reports/renewables-2022`.

[8] Serhan Cevik and Keitaro Ninomiya. "Chasing the Sun and Catching the Wind: Energy Transition and Electricity Prices in Europe". In: (2022).

[9] Tuomas Rintamäki, Afzal S Siddiqui, and Ahti Salo. "Does renewable energy generation decrease the volatility of electricity prices? An analysis of Denmark and Germany". In: *Energy Economics* 62 (2017), pp. 270–282.

[10] George Dantzig. *Linear programming and extensions*. Princeton university press, 1963.

[11] Laurence A Wolsey. *Integer programming*. Wiley, 1998.

[12] Robert J Vanderbei. *Linear Programming: Foundations and Extensions*. 3rd. Springer, 2014. ISBN: 9781461498157.

[13] Alexandr D Alexandrov. *Convex polyhedra*. Vol. 109. Springer, 2005.

[14] Ralph E Gomory. "Outline of an algorithm for integer solutions to linear programs". In: *Bulletin of the American Mathematical Society* 64.5 (Sept. 1958), pp. 275–278.

[15] Ailsa H Land and Alison G Doig. "An Automatic Method of Solving Discrete Programming Problems". In: *Econometrica* 28.3 (1960), pp. 497–520. ISSN: 00129682, 14680262. URL: `http://www.jstor.org/stable/1910129` (visited on 05/27/2023).

[16] Laurence A Wolsey. *Integer programming*. John Wiley & Sons, 2020.

[17] Cornell University Computational Optimization Open Textbook. "Heuristic algorithms". In: *Cornell University Computational Optimization Open Textbook* (2021). URL: https://optimization.cbe.cornell.edu/index.php?title=Heuristic_algorithms.

[18] John R Birge and François Louveaux. *Introduction to Stochastic Programming*. New York, NY: Springer Science & Business Media, 2011. DOI: 10.1007/978-1-4419-7338-2.

[19] Alan J King and Stein W Wallace. *Modeling with stochastic programming*. Springer Science & Business Media, 2012.

[20] Giovanni Pantuso. *Stochastic Programming - An introduction*. PowerPoint slides. 2022.

[21] Michal Kaut and Stein W Wallace. *Evaluation of scenario-generation methods for stochastic programming*. Humboldt-Universität zu Berlin, Mathematisch-Naturwissenschaftliche Fakultät ..., 2003.

[22] Jamie Fairbrother, Amanda Turner, and Stein W Wallace. "Problem-driven scenario generation: an analytical approach for stochastic programs with tail risk measure". In: *Mathematical Programming* (2022), pp. 1–42.

[23] Ralph T Rockafellar and Roger J-B Wets. "Scenarios and policy aggregation in optimization under uncertainty". In: *Mathematics of operations research* 16.1 (1991), pp. 119–147.

[24] Valentin Kaisermayer et al. "Progressive hedging for stochastic energy management systems". In: *Energy Systems* 12.1 (2021), pp. 1–29.

[25] Arne Løkketangen and David L Woodruff. "Progressive hedging and tabu search applied to mixed integer (0,1) multi-stage stochastic programming". In: *Journal of Heuristics* 2.2 (1996), pp. 111–128.

[26] Kalyanmoy Deb and Soumil Srivastava. "A genetic algorithm based augmented Lagrangian method for constrained optimization". In: *Computational optimization and Applications* 53.3 (2012), pp. 869–902.

[27] John M. Mulvey and Hercules Vladimirou. "Applying the progressive hedging algorithm to stochastic generalized networks". In: *Annals of Operations Research* 31 (1991), pp. 399–424.

[28] Shohre Zehtabian and Fabian Bastin. "Penalty Parameter Update Strategies in Progressive Hedging Algorithm". In: (Mar. 2016).

[29] Luckny Zéphyr and Bernard Lamond. "Adaptive monitoring of the progressive hedging penalty for reservoir systems management". In: *Energy Systems* (Dec. 2013). DOI: 10.1007/s12667-013-0110-4.

[30] Lars Magnus Hvattum and Arne Løkketangen. “Using scenario trees and progressive hedging for stochastic inventory routing problems”. In: *Journal of Heuristics* 15 (2009), pp. 527–557.

[31] Raphael EC Gonçalves, Erlon Cristian Finardi, and Edson Luiz da Silva. “Applying different decomposition schemes using the progressive hedging algorithm to the operation planning problem of a hydrothermal system”. In: *Electric power systems research* 83.1 (2012), pp. 19–27.

[32] Alexandre Oudalov, Rachid Cherkaoui, and Antoine Beguin. “Sizing and optimal operation of battery energy storage system for peak shaving application”. In: *2007 IEEE Lausanne Power Tech*. IEEE. 2007, pp. 621–625.

[33] Jeremy Neubauer and Mike Simpson. *Deployment of behind-the-meter energy storage for demand charge reduction*. Tech. rep. National Renewable Energy Lab.(NREL), Golden, CO (United States), 2015.

[34] Korosh Vatanparvar and Ratnesh Sharma. “Battery optimal approach to demand charge reduction in behind-the-meter energy management systems”. In: *2018 IEEE Power & Energy Society General Meeting (PESGM)*. IEEE. 2018, pp. 1–5.

[35] Frida Berglund et al. “Optimal operation of battery storage for a subscribed capacity-based power tariff prosumer—A Norwegian case study”. In: *Energies* 12.23 (2019), p. 4450.

[36] R Hanna et al. “Energy dispatch schedule optimization for demand charge reduction using a photovoltaic-battery storage system with solar forecasting”. In: *Solar Energy* 103 (2014), pp. 269–287.

[37] Jeremy Neubauer. *Battery lifetime analysis and simulation tool (BLAST) documentation*. Tech. rep. National Renewable Energy Lab.(NREL), Golden, CO (United States), 2014.

[38] Luis T Youn and Sohyung Cho. “Optimal operation of energy storage using linear programming technique”. In: *Proceedings of the World Congress on Engineering and Computer Science*. Vol. 1. 2009, pp. 480–485.

[39] Enrico Telaretti, Mariano Ippolito, and Luigi Dusonchet. “A simple operating strategy of small-scale battery energy storages for energy arbitrage under dynamic pricing tariffs”. In: *Energies* 9.1 (2015), p. 12.

[40] Abubakar Sani Hassan, Liana Cipcigan, and Nick Jenkins. “Optimal battery storage operation for PV systems with tariff incentives”. In: *Applied Energy* 203 (2017), pp. 422–441.

[41] Simon F Schneider, Petr Novák, and Tom Kober. "Rechargeable batteries for simultaneous demand peak shaving and price arbitrage business". In: *IEEE Transactions on Sustainable Energy* 12.1 (2020), pp. 148–157.

[42] Faeza Hafiz et al. "Real-time stochastic optimization of energy storage management using deep learning-based forecasts for residential PV applications". In: *IEEE Transactions on Industry Applications* 56.3 (2020), pp. 2216–2226.

[43] Agustín A. Sánchez de la Nieta et al. "Optimal midterm peak shaving cost in an electricity management system using behind customers' smart meter configuration". In: *Applied Energy* 283 (2021), p. 116282. ISSN: 0306-2619. DOI: https://doi.org/10.1016/j.apenergy.2020.116282. URL: https://www.sciencedirect.com/science/article/pii/S0306261920316706.

[44] BKK. *Nettleie for bedriftskunder*. [Accessed on 15.03.23]. URL: https://www.bkk.no/alt-om-nettleie/nettleie-for-bedriftskunder#2c344ad7c829.

[45] Volte. *Spotpris*. [Accessed on 5.12.22]. URL: https://www.volte.no/spotpris.

[46] Thomas Huld, Richard Müller, and Attilio Gambardella. "A new solar radiation database for estimating PV performance in Europe and Africa". In: *Solar Energy* 86.6 (2012), pp. 1803–1815.

[47] Norwegian Meteorological Institute. *seklima.no*. https://seklima.met.no/. Online database. 2023.

[48] Marie Bessec and Julien Fouquau. "The non-linear link between electricity consumption and temperature in Europe: A threshold panel approach". In: *Energy Economics* 30.5 (2008), pp. 2705–2721.

[49] Foad H Gandoman et al. "Short-term solar power forecasting considering cloud coverage and ambient temperature variation effects". In: *Renewable Energy* 123 (2018), pp. 793–805.

[50] Norges vassdrags- og energidirektorat (NVE). *Tariffer for Plusskunder*. Retrieved from https://www.nve.no/reguleringsmyndigheten/regulering/nettvirksomhet/nettleie/tariffer-for-produksjon/plusskunder/. Last updated on January 18, 2023. 2023.

[51] The scikit-garden contributors. *scikit-garden: Quantile Regression Forests in Python*. https://scikit-garden.github.io/api/#skgardenquantile_1. 2023.

[52] F. Pedregosa et al. "Scikit-learn: Machine Learning in Python". In: *Journal of Machine Learning Research* 12 (2011), pp. 2825–2830.

[53] Spyridon Chapaloglou et al. “Data-driven energy management of isolated power systems under rapidly varying operating conditions”. In: *Applied Energy* 314 (2022), p. 118906.

[54] Kristina Šutiene, Dalius Makackas, and Henrikas Pranevičius. “Multistage K-Means Clustering for Scenario Tree Construction”. In: *Informatica* 21.1 (2010), pp. 123–138.

[55] Albert Madansky. “Inequalities for stochastic linear programming problems”. In: *Management science* 6.2 (1960), pp. 197–204.

[56] Gurobi Optimization, LLC. *Gurobi Optimizer Reference Manual*. 2023. URL: `https://www.gurobi.com`.

A Progressive Hedging Algorithm

Algorithm 1 PHA

1: Set the iteration counter $k \leftarrow 0$, the initial penalty parameter $\rho^{(0)} \leftarrow \rho_0$

2: **for all** $s \in \mathcal{S}$ **do**

3: Solve the scenario subproblem:

$$\textbf{find } (x_{t,s}^{(0)})_{t\in\mathcal{T}} \in \arg\min \sum_{t\in\mathcal{T}} c_{t,s}^{\mathsf{T}} x_{t,s}$$
$$\text{subject to } W_{1,s}x_{1,s} = h_{1,s}, W_{t,s}x_{t,s} + T_{t-1,s}x_{t-1,s} = h_{t,s}, x_{t,s} \in X$$

4: **end for**

5: Compute the initial solution $\bar{x}_{\omega,t}^{(0)} \leftarrow \sum_{s\in\omega} \frac{p_s x_{t,s}^{(0)}}{\sum_{s\in\omega} p_s}$ and the initial duals $\lambda_{t,s}^{(0)} \leftarrow \rho^{(0)}(x_{t,s}^{(0)} - \bar{x}_{t,\omega}^{(0)})$ for all $s \in \omega, \omega \in \Omega_t, t \in \mathcal{T}$

6: **repeat**

7: **for all** $s \in \mathcal{S}$ **do**

8: Solve the augmented scenario subproblem:

$$\textbf{find } (x_{t,s}^{(k+1)})_{t\in\mathcal{T}} \in \arg\min \sum_{t\in\mathcal{T}} c_{t,s}^{\mathsf{T}} x_{t,s} + (\lambda_{t,s}^{(k)})^{\mathsf{T}} x_{t,s} + \frac{\rho^{(k)}}{2} \|x_{t,s} - \bar{x}_{t,\omega}^{(k)}\|_2^2$$
$$\text{subject to } W_{1,s}x_{1,s} = h_{1,s}, W_{t,s}x_{t,s} + T_{t-1,s}x_{t-1,s} = h_{t,s}, x_{t,s} \in X$$

9: **end for**

10: **for all** $\omega \in \Omega_t, t \in \mathcal{T}$ **do**

11: Update the solution $\bar{x}_{t,\omega}^{(k+1)} \leftarrow \sum_{s\in\omega} \frac{p_s x_{t,s}^{(k+1)}}{\sum_{s\in\omega} p_s}$

12: **end for**

13: **for all** $s \in \omega, \omega \in \Omega_t, t \in \mathcal{T}$ **do**

14: Update the duals $\lambda_{t,s}^{(k+1)} \leftarrow \lambda_{t,s}^{(k)} + \rho^{(k+1)}(x_{t,s}^{(k+1} - \bar{x}_{t,\omega}^{(k+1)})$

15: **end for**

16: $k \leftarrow k + 1$

17: **until** $\sum_{s\in\mathcal{S}} \sum_{t\in\mathcal{T}} p_s ||x_{t,s}^{(k+1)} - \bar{x}_{t,\omega}^{(k+1)}|| \leq \delta$ **or** $k > k_{\max}$

B Deterministic Model

$$\min \quad \sum_{m\in\mathcal{M}} \left(W_m l_m + \sum_{t\in\mathcal{T}_m} Q_{t,m}(x^{GD}_{t,m} + x^{GB}_{t,m}) - \sum_{t\in\mathcal{T}_m} K_{t,m}(x^{BG}_{t,m} + x^{EG}_{t,m}) \right)$$

$$\begin{aligned}
\text{s.t.} \quad & r_{t+1,m} = r_{t,m} + x^{EB}_{t,m} + x^{GB}_{t,m} - x^{BD}_{t,m} - x^{BG}_{t,m} && \forall t \in \mathcal{T}_m \setminus \{|\mathcal{T}_m|\}, \forall m \in \mathcal{M} \\
& r_{1,m} = r_{|\mathcal{T}_m|,m-1} + x^{EB}_{|\mathcal{T}_m|,m-1} + x^{GB}_{|\mathcal{T}_m|,m-1} - x^{BD}_{|\mathcal{T}_m|,m-1} - x^{BG}_{|\mathcal{T}_m|,m-1} && \forall m \in \mathcal{M} \\
& x^{ED}_{t,m} + x^{BD}_{t,m} + x^{GD}_{t,m} = D_{t,m} && \forall t \in \mathcal{T}_m, \forall m \in \mathcal{M} \\
& x^{EG}_{t,m} + x^{EB}_{t,m} + x^{ED}_{t,m} \leq e_{t,m} && \forall t \in \mathcal{T}_m, \forall m \in \mathcal{M} \\
& x^{GB}_{t,m} + x^{EB}_{t,m} \leq B \cdot \mu_{t,m} && \forall t \in \mathcal{T}_m, \forall m \in \mathcal{M} \\
& x^{BD}_{t,m} + x^{BG}_{t,m} \leq B \cdot (1 - \mu_{t,m}) && \forall t \in \mathcal{T}_m, \forall m \in \mathcal{M} \\
& x^{BG}_{t,m} + x^{EG}_{t,m} \leq M \cdot \pi_{t,m} && \forall t \in \mathcal{T}_m, \forall m \in \mathcal{M} \\
& x^{GD}_{t,m} + x^{GB}_{t,m} \leq M \cdot (1 - \pi_{t,m}) && \forall t \in \mathcal{T}_m, \forall m \in \mathcal{M} \\
& x^{EG}_{t,m} + x^{BG}_{t,m} \leq \min(A, F) && \forall t \in \mathcal{T}_m, \forall m \in \mathcal{M} \\
& x^{GD}_{t,m} + x^{GB}_{t,m} \leq l_m && \forall t \in \mathcal{T}_m, \forall m \in \mathcal{M} \\
& r_{t,m} \leq B && \forall t \in \mathcal{T}_m, \forall m \in \mathcal{M} \\
& r_{1,1} = 0 \\
& \mu_{t,m} \in \{0,1\} && \forall t \in \mathcal{T}_m, \forall m \in \mathcal{M} \\
& \pi_{t,m} \in \{0,1\} && \forall t \in \mathcal{T}_m, \forall m \in \mathcal{M} \\
& x^{GD}_{t,m}, x^{BD}_{t,m}, x^{BG}_{t,m}, x^{GB}_{t,m} x^{EB}_{t,m}, x^{ED}_{t,m} x^{EG}_{t,m}, r_{t,m} \geq 0, && \forall t \in \mathcal{T}_m, \forall m \in \mathcal{M}
\end{aligned}$$

Table 9: Description of parameters, sets, and decision variables of the deterministic model

Symbol	Description
Parameters	
$Q_{t,m}$	Price for buying electricity
$K_{t,m}$	Revenue for selling electricity
$E_{t,m}$	Electricity generated from PV system
$D_{t,m}$	Demand for electricity
W_m	Demand charge
B	Size of battery
F	Electrical installation capacity
A	Maximum grid injection
M	A very large number
Sets	
$\mathcal{T}_m$	Set of hours
$\mathcal{M}$	Set of months
Decision Variables	
$x_{t,m}^{ED}$	Flow of energy from PV system to demand
$x_{t,m}^{EB}$	Flow of energy from PV system to battery
$x_{t,m}^{EG}$	Flow of energy from PV system to grid
$x_{t,m}^{GD}$	Flow of energy from grid to demand
$x_{t,m}^{GB}$	Flow of energy from grid to battery
$x_{t,m}^{BG}$	Flow of energy from battery to grid
$x_{t,m}^{BD}$	Flow of energy from battery to demand
$r_{t,m}$	Energy in battery during hour t and month m
l_m	Peak demand
$\mu_{t,m}$	Binary variable. 1 when battery storage is charging, 0 otherwise
$\pi_{t,m}$	Binary variable. 1 when selling to the grid, 0 otherwise

C Complete Stochastic Model

$$\min \quad \sum_{s\in\mathcal{S}} p_s \Bigg(\sum_{m\in\mathcal{M}} \Bigg(W_{m,s} l_{m,s} + \sum_{t\in\mathcal{T}_m} Q_{t,m,s}(x^{GD}_{t,m,s} + x^{GB}_{t,m,s} + \beta_{t,m,s}) - \sum_{t\in\mathcal{T}_m} K_{t,m,s}(x^{BG}_{t,m,s} + x^{EG}_{t,m,s} + \alpha_{t,m,s}) \Bigg) \Bigg)$$

$$\text{s.t.} \quad r_{t+1,m,s} = r_{t,m,s} + x^{EB}_{t,m,s} + x^{GB}_{t,m,s} - x^{BD}_{t,m,s} - x^{BG}_{t,m,s} \qquad \forall t \in \mathcal{T}_m \setminus |T|, \forall m \in \mathcal{M}, \forall s \in \mathcal{S}$$

$$r_{1,m,s} = r_{|T|,m-1,s} + x^{EB}_{|T|,m-1,s} + x^{GB}_{|T|,m-1,s} - x^{BD}_{|T|,m-1,s} - x^{BG}_{|T|,m-1,s} \qquad \forall t \in \mathcal{T}_m, \forall m \in \mathcal{M}, \forall s \in \mathcal{S}$$

$$x^{ED}_{t,m,s} + x^{GD}_{t,m,s} + x^{BD}_{t,m,s} = \xi^{D}_{t,m}(s) + \alpha_{t,m,s} \qquad \forall t \in \mathcal{T}_m, \forall m \in \mathcal{M}, \forall s \in \mathcal{S}$$

$$x^{EB}_{t,m,s} + x^{ED}_{t,m,s} + x^{EG}_{t,m,s} \leq \xi^{E}_{t,m}(s) + \beta_{t,m,s} \qquad \forall t \in \mathcal{T}_m, \forall m \in \mathcal{M}, \forall s \in \mathcal{S}$$

$$x^{GB}_{t,m,s} + x^{EB}_{t,m,s} \leq B \cdot \mu_{t,m,s} \qquad \forall t \in \mathcal{T}_m, \forall m \in \mathcal{M}, \forall s \in \mathcal{S}$$

$$x^{BD}_{t,m,s} + x^{BG}_{t,m,s} \leq B \cdot (1 - \mu_{t,m,s}) \qquad \forall t \in \mathcal{T}_m, \forall m \in \mathcal{M}, \forall s \in \mathcal{S}$$

$$x^{BG}_{t,m,s} + x^{EG}_{t,m,s} \leq M \cdot \pi_{t,m,s} \qquad \forall t \in \mathcal{T}_m, \forall m \in \mathcal{M}, \forall s \in \mathcal{S}$$

$$x^{GD}_{t,m,s} + x^{GB}_{t,m,s} \leq M \cdot (1 - \pi_{t,m,s}) \qquad \forall t \in \mathcal{T}_m, \forall m \in \mathcal{M}, \forall s \in \mathcal{S}$$

$$x^{EG}_{t,m,s} + x^{BG}_{t,m,s} + \alpha_{t,m,s} \leq \min(A, F) \qquad \forall t \in \mathcal{T}_m, \forall m \in \mathcal{M}, \forall s \in \mathcal{S}$$

$$x^{GD}_{t,m,s} + x^{GB}_{t,m,s} + \beta_{t,m,s} \leq l_{m,s} \qquad \forall t \in \mathcal{T}_m, \forall m \in \mathcal{M}, \forall s \in \mathcal{S}$$

$$x^{GB}_{t,m,s_1} = x^{GB}_{t,m,s_2} \qquad \forall s_1, s_2 \in \omega, \forall \omega \in \Omega_t, \forall t \in \mathcal{T}_m, \forall m \in \mathcal{M}$$

$$x^{BG}_{t,m,s_1} = x^{BG}_{t,m,s_2} \qquad \forall s_1, s_2 \in \omega, \forall \omega \in \Omega_t, \forall t \in \mathcal{T}_m, \forall m \in \mathcal{M}$$

$$x^{BD}_{t,m,s_1} = x^{BD}_{t,m,s_2} \qquad \forall s_1, s_2 \in \omega, \forall \omega \in \Omega_t, \forall t \in \mathcal{T}_m, \forall m \in \mathcal{M}$$

$$x^{EB}_{t,m,s_1} = x^{EB}_{t,m,s_2} \qquad \forall s_1, s_2 \in \omega, \forall \omega \in \Omega_t, \forall t \in \mathcal{T}_m, \forall m \in \mathcal{M}$$

$$x^{ED}_{t,m,s_1} = x^{ED}_{t,m,s_2} \qquad \forall s_1, s_2 \in \omega, \forall \omega \in \Omega_t, \forall t \in \mathcal{T}_m, \forall m \in \mathcal{M}$$

$$r_{t,m,s} \leq B \qquad \forall t \in \mathcal{T}_m, \forall m \in \mathcal{M}, \forall s \in \mathcal{S}$$

$$r_{1,1} = 0$$

$$\mu_{t,m,s} \in \{0, 1\} \qquad \forall t \in \mathcal{T}_m, \forall m \in \mathcal{M}, \forall s \in \mathcal{S}$$

$$\pi_{t,m,s} \in \{0, 1\} \qquad \forall t \in \mathcal{T}_m, \forall m \in \mathcal{M}, \forall s \in \mathcal{S}$$

$$x^{GD}_{t,m,s}, x^{BD}_{t,m,s}, x^{BG}_{t,m,s}, x^{GB}_{t,m,s} x^{EB}_{t,m,s}, x^{ED}_{t,m,s} x^{EG}_{t,m,s}, r_{t,m,s} \geq 0, \qquad \forall t \in \mathcal{T}_m, \forall m \in \mathcal{M}, \forall s \in \mathcal{S}$$

Table 10: Description of parameters, sets, and decision variables of the stochastic model

Symbol	Description
Parameters	
$Q_{t,m.s}$	Price for buying electricity
$K_{t,m,s}$	Revenue for selling electricity
$E_{t,m,s}$	Electricity generated from PV system
$D_{t,m,s}$	Demand for electricity
$W_{m,s}$	Demand charge
p_s	Probability of scenario s occurring
B	Size of battery
F	Electrical installation capacity
A	Maximum grid injection
M	A very large number
Sets	
$\mathcal{T}_m$	Set of hours in month m
$\mathcal{M}$	Set of months
$\mathcal{S}$	Set of scenarios
ω	Set of equivalent scenarios
Ω_t	Set of ω in time t
First Stage Decision Variables	
$x^{ED}_{t,m,s}$	Flow of energy from PV system to demand
$x^{EB}_{t,m,s}$	Flow of energy from PV system to battery
$x^{GB}_{t,m,s}$	Flow of energy from grid to battery
$x^{BG}_{t,m,s}$	Flow of energy from battery to grid
$x^{BD}_{t,m,s}$	Flow of energy from battery to demand
$r_{t,m,s}$	Energy in battery
$\mu_{t,m,s}$	Binary variable. 1 when battery storage is charging, 0 otherwise
$\pi_{t,m,s}$	Binary variable. 1 when selling to the grid, 0 otherwise

Recourse Decision Variables

$x^{GD}_{t,m,s}$	Shortfall of planned energy relative to demand
$\alpha_{t,m,s}$	Overestimation of planned energy relative to demand
$x^{EG}_{t,m,s}$	Underestimation of planned solar power production
$\beta_{t,m,s}$	Overestimation of planned solar power production
l_m	Peak demand

D Case study 1 results

Table 11: Cost and Revenue without Battery

Month	Cost of energy bought from the grid	Revenue from selling energy to the grid	Peak demand cost
1	61015	0	4823
2	51949	0	4885
3	63743	50	4377
4	47145	249	3602
5	48148	536	3442
6	45742	227	4055
7	41718	472	4493
8	95062	310	5020
9	91270	337	3723
10	45329	0	4146
11	38069	0	4148
12	107154	0	5071

Table 12: Cost and Revenue with Battery

Month	Cost of energy bought from the grid	Revenue from selling energy to the grid	Peak demand cost
1	60173	74	3803
2	51538	66	3619
3	62247	946	3345
4	46631	1058	2707
5	45962	415	2632
6	43922	342	3007
7	40307	291	2827
8	95215	3843	3866
9	88749	6672	3625
10	42571	476	3598
11	35913	135	3165
12	103636	1038	4215